Resonance tongue interaction in the parametrically excited column

A.R. Champneys [1]
Department of Engineering Mathematics,
Queens Building,
University of Bristol,
Bristol BS8 1TR, UK.

and

W.B. Fraser
School of Mathematics and Statistics,
The University of Sydney,
NSW 2006, Australia.

Submitted to *SIAM J. App. Math.* November 22, 2002

[1]Corresponding author A.R. Champneys@bris.ac.uk

Abstract

This paper concerns a codimension-two analysis of the interaction between various resonances that occur in an upright flexible rod subject to sinusoidal parametric excitation. Particular attention is paid to rods that are just longer than their critical length for self-weight buckling, and their possible stabilization by the excitation. Previous work has identified three small dimensionless parameters in this problem; the closeness of the length (divided by the cube root of bending stiffness) to the critical one, the amplitude of excitation, and the reciprocal of the frequency of excitation. Multiple time-scale analysis is used to show how the asymptotics of resonance tongues in the amplitude-versus-bending-stiffness plane becomes of lower-order at certain special values of the frequency ratio where two resonances interact. In particular, an $O(1)$ change in the shape of the parameter region of the stabilised supercritical rod occurs through interaction with the pure harmonic resonance of some other mode of vibration of the rod. It is also shown how to include material damping within the analysis. The results help explain why earlier theories failed to qualitatively explain experimental observation, and are also likely to be of relevance in other 3-parameter parametric resonance problems for continuous structures.

1 Introduction

It is well known that if a column exceeds a certain critical length it will, when placed upright, buckle under its own weight. A recent experiment by Mullin, reported in Mullin, Fraser, Galan & Acheson (2002) (see also Acheson (1997) and Acheson & Mullin (1998)) has demonstrated that a piece of 'curtain wire' that is longer than its critical length can be stabilised by subjecting its bottom support point to a vertical vibration of appropriate amplitude and frequency. In two previous papers, (Champneys & Fraser 2000, Fraser & Champneys 2002) henceforth referred to as Part I and Part II respectively, we made a numerical and asymptotic study of the linear and nonlinear equations that govern the behaviour of such a column.

In Part I it was noted that there are three key dimensionless parameters in this problem: B the ratio of the column's bending stiffness to the cube of its length; η (called $1/\delta$ in that paper) the square of the ratio of the frequency of excitation to that of the pendulum of the same length ($\sqrt{g/\ell}$); and ε, the amplitude of excitation. By looking in the (B, ε) plane for fixed η, one can then analyse the stability of the upright position using Floquet analysis and double scale asymptotics, in much the same way as one does for the single degree of freedom Mathieu equation (e.g. Jordan & Smith (1986), Nayfeh & Mook (1979)). The result for the fundamental instability curve is to show that for 'most' η-values it is possible to stabilize, for small ε, a column that is just longer ($B < B_c$) than its critical length for self-weight buckling. In fact, this criterion gives a lower bound on the frequency of excitation that is required in order to stabilize a column of a given length. However, this lower bound is too conservative when compared with experiments, (Mullin et al. 2002). Nor does it give the observed upper bound.

Part II concerns an attempt to answer these deficiencies by considering, in addition, harmonic and sub-harmonic instabilities. In that paper the analysis was also extended to include a fully geometrically nonlinear formulation, but the ensuing weakly nonlinear asymptotic analysis in essence held no surprises. However, it was observed that the quadratic-in-ε coefficient of the B-value bounding the fundamental stability region can undergo singularities as η varies. These occur precisely when a first harmonic resonance has the same B-value as the self-weight buckling $B = B_c$. In fact, in the analyses of both the fundamental and harmonic instabilities, the asymptotic expansions became invalid at these special values of the excitation frequency. This breakdown appears to be an artifact of the particular expansions used there. In this paper we offer an alternative expansion

procedure that avoids this difficulty.

The key is to think of this as a genuinely three-parameter problem, and expand both B and η in powers of ε in a neighbourhood of these codimension-two *resonance-tongue interaction* points. In what follows we shall consider only the linear equations of motion of the column, since the tongue interaction we wish to describe involves the (loss of) linear stability of an upright column. As in part II, the results can be extended to include geometrically nonlinear terms, to give the amplitude and stability of the bifurcating motion. But, since our prime objective is to describe the shape of stability regions in a neighbourhood of codimension-two points, we shall omit such complications here.

The rest of the paper is outlined as follows. Section 2 contains a brief review of the mathematical formulation, and some new insight into the behaviour of eigenmodes and resonances as parameters are varied. Section 3 then considers the possibility of two instabilities occuring at once, and introduces a general asymptotic expansion procedure for unfolding such a situation. It is argued how only a few of these interactions lead to a qualitatively significant change in the stability regions, including the case where there is a singularity in the coefficient of the sub-harmonic resonance boundary (with dimensionless frequency 1/2), due to its interaction with the tongue corresponding to frequency 3/2. Section 4 then studies the important special case where the fundamental buckling instability interacts with a first harmonic resonance of any one of the higher-order eigenmodes. Section 5 shows how the results are modified in the presence of damping. Section 6 compares the analysis of this paper to the results of the curtain wire experiments, and finally Sect. 7 draws conclusions and discusses the results in a wider context.

2 Mathematical Formulation

Consider an initially straight column of length ℓ, with a uniform circular cross-section of radius $a \ll \ell$ and mass linear density m per unit length (see Fig. 1). The column is assumed to be inextensible, unshearable and linearly elastic with bending stiffness $\bar{B}$. It is further assumed that the lower end is clamped upright and is displaced by a vertical harmonic oscillation equal to $\Delta \cos \omega_0 \bar{t}$. The upper end is assumed to be free. The derivation of the geometrically nonlinear equations that govern the motion of the centreline $\bar{\mathbf{R}}(\bar{s}, \bar{t})$, and tension $\bar{T}(\bar{s})$ of such a column was detailed in Parts I and II.

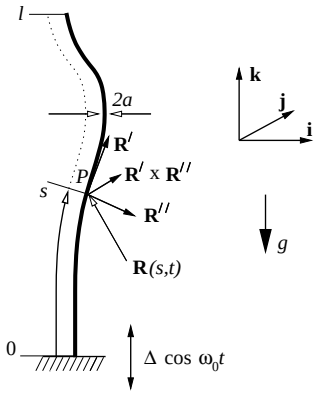

Figure 1: Definition sketch

There it was shown that the effects of rotary inertia and torsional waves in the angular momentum equation can be neglected Also, in Galan, Fraser, Acheson & Champneys (2002) it is shown, via homogenisation of a system of links with stiff damped joints, how to include a dimensionless coefficient of material damping Γ into the linearised equations.

2.1 Linearised equations

The dimensionless form of the linearized equations and boundary conditions governing small amplitude motion $\mathbf{r}(s,t)$ of the column about the oscillating upright position are [c.f. Part II eqs. (2.5) (2.6) and (2.7)]:

$$\eta\left\{\gamma \mathrm{D}\mathbf{r}^{IV} + \mathrm{D}^2\mathbf{r} - \varepsilon\cos t[(1-s)\mathbf{r}']'\right\} = -\mathcal{M}\mathbf{r} + T'\mathbf{k}, \tag{2.1}$$

where $()' = d/ds$, $D = d/dt$ and

$$\mathcal{M}\mathbf{r} := B\mathbf{r}^{IV} + [(1-s)\mathbf{r}']', \qquad \text{subject to} \tag{2.2}$$

$$\mathbf{r} = \mathbf{r}' = \mathbf{0}, \text{ at } s = 0; \quad \mathbf{r}'' = \mathbf{r}''' = \mathbf{0}, \ T = 0, \text{ at } s = 1, \tag{2.3}$$

Furthermore, inextensibility implies

$$\mathbf{r}' \cdot \mathbf{k} = 0. \tag{2.4}$$

The dimensionless variables are defined in terms of the dimensional (barred) variables by the following relations:

$$\left.\begin{aligned} s = \frac{\bar{s}}{\ell}, \quad \mathbf{r} = \frac{\bar{\mathbf{R}}}{\ell} - (\varepsilon\cos t + s)\mathbf{k}, \quad t = \omega_0\bar{t}, \quad \gamma = \tfrac{\Gamma\ell\omega}{mg} \\ T = \frac{\bar{T}}{mg\ell} - (1-\eta\varepsilon\cos t)(1-s), \quad B = \frac{\bar{B}}{mg\ell^3}, \quad \eta = \frac{\omega_0^2\ell}{g}, \quad \varepsilon = \tfrac{\Delta}{\ell}. \end{aligned}\right\} \tag{2.5}$$

In fact, we can eliminate T immediately by considering the $\mathbf{k}$ component of eq. (2.1) subject to condition (2.4), which gives the result $T \equiv 0$. Moreover, without loss of generality at this linearised level we can assume that the motion is restricted to the $(\mathbf{i}, \mathbf{k})$-plane and write $\mathbf{R}(s,t) = u(s,t)\mathbf{i}$ where u satisfies the scalar inhomegenious, parametrically forced linear PDE

$$\mathrm{M}u + \eta\left\{\gamma \mathrm{D}u^{IV} + \mathrm{D}^2 u - \varepsilon\cos t[(1-s)u']'\right\} = 0\,, \tag{2.6}$$

where

$$\mathrm{M}u := Bu^{IV} + [(1-s)u']' := Bu^{IV} + \mathrm{L}u, \qquad \text{subject to} \tag{2.7}$$

$$u = u' = 0, \text{ at } s = 0; \quad u'' = u''' = 0 \text{ at } s = 1. \tag{2.8}$$

This completes the formulation of the linear stability problem for the vertically oscillated column. For the majority of this paper we shall consider the perfect rod without the presence of material damping.

2.2 Eigenmodes of the unforced, undamped problem.

Consider $\varepsilon = \gamma = 0$. This is the unforced problem. The general linear solution for a given B-value is a superposition of eigenmodes

$$\sum_n \left\{A_n \cos\sqrt{\lambda_n/\eta_n}\, t + B_n g_n \sin\sqrt{\lambda_n/\eta_n}\, t\right\}\phi_n(s;B)$$

where ϕ_n is the eigenmode of M corresponding to λ_n. That is, (ϕ_n, λ_n) satisfy

$$\mathrm{M}\phi_n - \lambda_n\phi_n = 0, \tag{2.9}$$

together with boundary conditions (2.8). Note that for each B-value the operator M is self-adjoint and so the eigenfunctions form a complete orthonormal basis for L^2 subject to the boundary conditions (2.8), where we choose to normalise each eigenfunction such that their L^2-norm is unity. Then, upon defining

$$\langle a, b\rangle = \int_0^1 a(s)b(s)ds,$$

we have

$$\langle\phi_i, \phi_j\rangle = \delta_{i,j}, \quad \langle\phi_i, \mathrm{M}\phi_j\rangle = \lambda_j\delta_{i,j}, \tag{2.10}$$

and

$$\langle\phi_i^{IV}, v\rangle = \langle\phi_i'', v''\rangle, \quad \langle\phi_i, \mathrm{L}v\rangle = \langle v, \mathrm{L}\phi_i\rangle = -B\langle\phi_i'', v''\rangle + \lambda_i\langle\phi_i, v\rangle, \tag{2.11}$$

for any function $v(s)$ satisfying the boundary conditions (2.8). Here

$$\mathrm{L}v(s) := [(1-s)v'' - v']. \tag{2.12}$$

These identities will prove useful in what follows.

Now the eigenmodes $\phi_n(s;B)$ are in general not expressible in closed form except at the special values of B at which $\lambda_n(B) = 0$, in which case (see Part II, sect. 3), there is a solution in terms of the Bessel function $J_{-1/3}$. The same analysis shows that there are infinitely many such B-values, $B_{0,n}$ $n = 1, 2, 3, 4, \ldots$, accumulating at $B = 0$, the first few values of which are $B_{0,1} = 0.127594$, $B_{0,2} = 0.017864$, $B_{0,3} = 0.0067336$ and $B_{0,4} = 0.0003503$. These correspond respectively to where each eigenvalue locus $\lambda_n(B)$, for $n = 1, 2, 3, 4$, crosses the B-axis, with the corresponding eigenmode there having $n-1$ internal zeros. The lowering of B through each $B_{0,n}$-value implies that the nth mode becomes linearly unstable. Hence for $B > B_c := B_{0,1}$ the unforced rod is stable to self-weight buckling (a result known to Greenhill (1881)). Numerically, in Part I it was found that each eigenmode $\phi_n(s)$ retains a qualitatively similar mode shape for $B > B_{0,n}$ and that the corresponding loci $\lambda_n(B)$ are approximately straight lines (see Part I, Fig. 2, and the schematic diagram in the upper part of Fig. 2 below). In fact, we can now identify the slopes of those lines via the following asymptotic analysis.

Consider a rod for a specific length $B = B_0$ with eigenvalue and eigenmode $(\lambda_n,\ \phi_n)$ for some n. Let us expand in a small parameter δ via

$$B = B_0 + \delta B_1, \qquad \phi = \phi_n + \delta f_1 + \delta^2 f_2 + \ldots,$$

$$\lambda = \lambda_n + \delta\sigma_1 + \delta^2\sigma_2 + \ldots.$$

Taking these expansions and substituting them into the eigenvalue equation (2.9), and collecting powers of δ, we obtain

$$(\mathrm{M}_0 - \lambda_n)f_1 = -B_1\phi_n^{IV} + \sigma_1\phi_n \tag{2.13}$$

$$(\mathrm{M}_0 - \lambda_n)f_2 = -B_1 f_1^{IV} + \sigma_1 f_1 + \sigma_2\phi_n, \tag{2.14}$$

where M_0 is the operator M evaluated at $B = B_0$. The solvability condition for the $O(\delta)$ equation is that the right-hand side of (2.13) should be orthogonal to the eigenfunction ϕ_n of the left-hand side. Using the identity $(2.11)_1$ this yields

$$\sigma_1 = B_1\langle\phi_n'', \phi_n''\rangle \quad \text{and } \langle f_1, \phi_n\rangle = 0.$$

At the next order, the same solvability condition applied to eq. (2.14) yields

$$\sigma_2 = B_1 \langle \phi_n'', f_1'' \rangle$$

where f_1 is the solution of

$$\mathrm{M}_0 f_1 - \lambda_n f_1 = \sigma_1 \left(\phi_n - \frac{1}{\langle \phi_n'', \phi_n'' \rangle} \phi_n^{IV} \right), \tag{2.15}$$

subject to the boundary conditions (2.8). Combining these results we obtain the following asymptotic expression for dependence of any eigenvalue on B:

$$\lambda = \lambda_n + \delta B_1 \langle \phi_n'', \phi_n'' \rangle + \delta^2 B_1 \langle \phi_n'', f_1'' \rangle + O(\delta^3), \tag{2.16}$$

where we have used explicitly $\langle \phi_n, \phi_n \rangle = 1$. Note that the linear term is a positive definite quantity for all B. Hence the slopes of the loci $\lambda(B)$ are strictly positive for all n and B. This proves a property that was observed only numerically in Part I. In fact, we found there numerically that for $\lambda_n(B) > 0$ the locus is in fact well approximated by a straight line.

2.3 Dynamic resonances

Consider now the parametrically excited problem $\varepsilon \neq 0$. It is not difficult to see that in the limit $\varepsilon \to 0$, the dimensionless drive angular frequency η will be in resonance with a natural vibration frequency λ_n whenever $\lambda_n(B) = p^2 \eta$ for some $n > 0$, $p \geq 0$. Such B-values we label as $B = B_{p,n}$. Similarly, sub-harmonic resonances occur in the limit $\varepsilon \to 0$ at points $B = B_{p/2,n}$ defined for odd integers p such that $\lambda_n(B) = p^2 \eta / 2$.

Using Floquet theory (see Part I) one can deduce that for $\varepsilon > 0$, each of these resonance points $B_{\alpha,n}$ for non-negative half-integers integers α is the root point of an instability tongue in the (B, ε)-plane (see Fig. 2). One branch of the tongue corresponds to neutral modes whose leading order term is $\phi_n(s) \cos \alpha t$ (in phase with the excitation) and the other to modes with leading order term $\phi_n(s) \sin \alpha t$ (out of phase with the excitation). The case $\alpha = 0$ is special. This corresponds to the instability resulting from one of the pure buckling modes. From such a root point $B = B_{0,n}$ there is thus a single curve corresponding to an instability whose mode shape is time independent to leading order. Figure 3 shows actual tongue boundaries in the (B, ε)-plane computed using the numerical Floquet theory method presented in Part I.

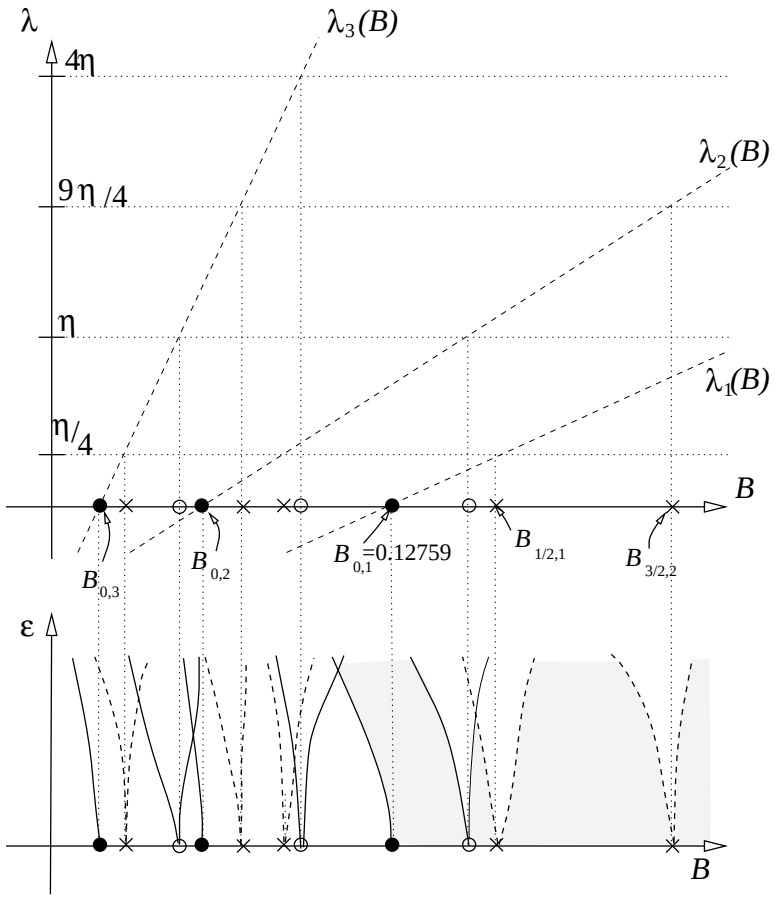

Figure 2: Summarizing schematically the results from Part I and the formula (2.17). The upper part shows eigenvalue loci $\lambda_n(B)$ and the definition of the points $B_{\alpha,n}$. In the lower part Instability tongues in the (B, ε)-plane are shown to occur with root points $B_{\alpha,n}$ and to have width $\varepsilon^{2\alpha}$. The shaded regions correspond to the where the vertical solution is stable. Solid lines represent neutral stability curves with Floquet multiplier $+1$ (where α is an integer) and dashed lines to multipliers -1 (where α is half an odd integer).

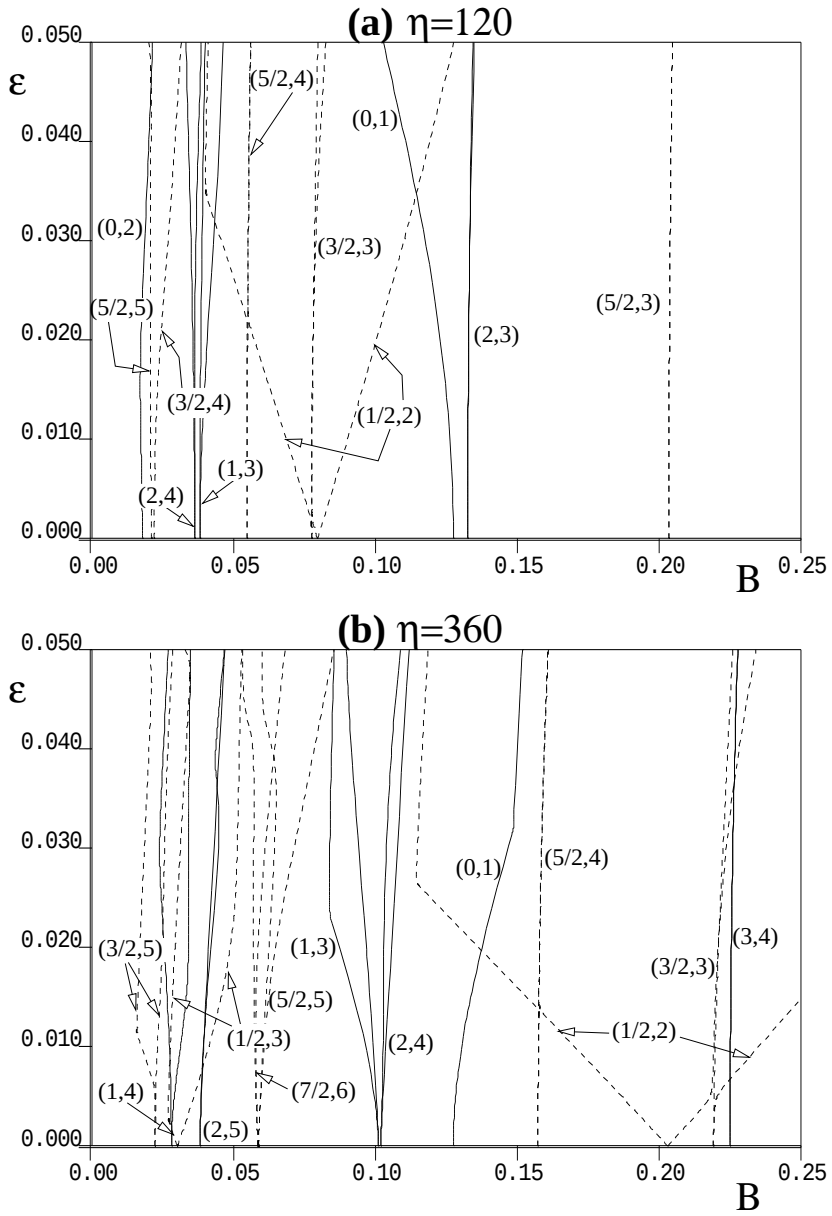

Figure 3: Resonance tongue boundaries computed using numerical Floquet analysis with $N = 4$ for (a) $\eta = 120$ and (b) $\eta = 360$. Depicted are all resonance tongues (labelled by (α, n)) with root points corresponding to $B_{\alpha,n}$ with $\alpha \leq 5/2$ and $n \leq 4$ and $0.02 < B < 0.25$. Note that the order of the resonance tongues changes between the figures (but the instability curve $(0, 2)$ is ommited from panel (b) for clarity). This is because at intermediate η-values there have been codimension-two resonance tongue interactions which form the subject of this paper. Note that each tongue other than the instability boundary coming out of $B_{0,n}$ has non-zero width which is sometimes not apparent on the scale depicted.

In fact, following the arguments laid out in section 3 below, we can add to this result. Specifically any instability with root point $B_{\alpha,n}$ which is a resonance whose neutral modes are like $\cos\alpha t$ or $\sin\alpha t$, leads to a tongue the boundaries of which are (under certain non-degeneracy assumptions) given by

$$B = B_{\alpha,m} + \sum_{j=2}^{2\alpha-1} B_j\,\varepsilon^j + B^{\pm}_{2\alpha}\,\varepsilon^{2\alpha}, \tag{2.17}$$

for some coefficients B_j and $B^{\pm}_{2\alpha}$. Here the superscript '+' represents a neutral stability curve corresponding to motion whose time variation is $\cos\alpha t$, i.e. in phase with the drive, and the superscript '$-$' corresponds to the neutral stability of out of phase motion whose time variation is $\sin\alpha t$.

Thus the simplest family of sub-harmonic resonances, corresponding to $\alpha = 1/2$, lead to linear instability tongues, whereas the simplest harmonic instability, corresponding to $\alpha = 1$, gives quadratic tongues. Higher-order tongues have width $\varepsilon^{2\alpha}$ albeit with a generically non-zero quadratic lean in the (B,ε)-plane. Thus $\alpha = 3/2$ leads to tongues with width $O(\varepsilon^3)$ in the (B,ε)-plane; $\alpha = 2$ leads to tongues with widths varying to the fourth power of ε, etc. Therefore, for small amplitude of excitation ε, only instabilities corresponding to lower values of α are likely to lead to any significant regions of instability provided the amplitude of excitation ε is small (an observation that further vindicated by the the presence of damping, see Sec. 5 below). The case $\alpha = 0$ is once again special, and it was shown in Part I that this leads to a single boundary between instability and stability that is to leading order quadratic in B.

The general result (2.17) confirms and extends what we found by detailed multiple timescale asymptotics in Parts I & II. Before proceeding to a codimension-two analysis of when the non-degeneracy conditions leading to (2.17) fail, let us extract from Part II the leading-order expressions for the coefficients in the simplest few cases.

Taking $\alpha = 0$, the single neutral curve is defined by

$$B = B_{0,n} + B_2\varepsilon^2 + O(\varepsilon^3)$$

where (Part II, eq. (4.11), interpreted in the notation of this paper)

$$B_2 = \frac{\eta\langle\phi_n, \mathrm{L}H_1\rangle}{2\langle\phi_n'', \phi_n''\rangle}, \tag{2.18}$$

with H_1 being the solution to

$$\mathrm{M}_{0,n}H_1 - \eta H_1 = \eta\mathrm{L}\phi_n \tag{2.19}$$

subject to the usual boundary conditions (2.8).

Taking $\alpha = 1/2$, the neutral stability curves are defined by

$$B = B_{1/2,n} + B_1^{\pm}\varepsilon + O(\varepsilon^2),$$

where (Part II, eq. (4.19))

$$B_1^{\pm} = \pm\frac{\eta\langle\phi_n, \mathrm{L}\phi_n\rangle}{2\langle\phi_n'', \phi_n''\rangle}. \tag{2.20}$$

In the case $\alpha = 1$, neutral stability occurs along the curves

$$B = B_{1,n} + B_2^{\pm}\varepsilon^2 + O(\varepsilon^3),$$

where (upon solving for $\alpha_1 = \pm\alpha_2$ in Part II, eq. (4.26))

$$B_2^{+} = \eta\frac{2\langle\phi_n, \mathrm{L}H_4\rangle + \langle\phi_n, \mathrm{L}H_3\rangle}{2\langle\phi_n'', \phi_n''\rangle}, \tag{2.21}$$

$$B_2^{-} = \frac{\eta\langle\phi_n, \mathrm{L}H_3\rangle}{2\langle\phi_n'', \phi_n''\rangle}, \tag{2.22}$$

with H_3 and H_4 being the solutions to

$$\mathrm{M}_{1,n}H_3 - 4\eta H_3 = \frac{\eta}{2}\mathrm{L}\phi_n, \tag{2.23}$$

$$\mathrm{M}_{1,n}H_4 = \frac{\eta}{2}\mathrm{L}\phi_n, \tag{2.24}$$

subject to the usual boundary conditions (2.8)

We now notice several anomalies from Fig. 3. First the instability curve $(0, 1)$ representing the fundamental falling-over instability, bends back to the left for $\eta = 120$, (as indeed it does for 'most' η-values, as was argued in Part I to explain the stabilization effect observed in the experiment). However for $\eta = 360$, this curve bends to the right, thus showing that increasing ϵ does not lead to a region of stability of the forced rod that failed to exist for the unforced problem. This anomaly forms the subject of Sec. 4 below. Second, the instability tongue $(1/2, 2)$ undergoes, for $\eta \approx 360$, a strange interaction process with the $(3/2, 3)$-tongue in the bottom right of the Fig. 3(b). An explanation of this and similar interactions forms the subject of section 4 below.

3 Resonance tongue interaction

The general expression (2.17) giving the leading-order expression for resonance tongues is subject to non-degeneracy conditions. These non-degeneracy conditions fail at special values of η for which

$$B_{\alpha,n} = B_{\beta,m} \quad \text{for} \quad n \neq m, \tag{3.1}$$

and values of α and β that are related by certain conditions as we shall now explain.

It was noted in Part II that the coefficient B_2 given by (2.18) becomes singular precisely when $\lambda_m = \eta$ is another eigenvalue of M, corresponding to eigenmode ϕ_m. That is, there is the coexistence of resonances (3.1) corresponding to $\alpha = 1$ and $\beta = 0$. We can see why this is so since the equation (2.19) becomes such that the left-hand side is solved by eigenfunction ϕ_m and hence the solution becomes unbounded unless the right-hand side function is orthogonal to ϕ_m. This will occur at a special pair of of values of (η_0, B_0) of η and B for which $M_0\phi_n = M_0\phi_m - \eta_0\phi_m = 0$. At such points we can see that the coefficient of the quadratic coefficient B_2^+ of the resonance tongue corresponding to $\phi_m \cos t$ also becomes unbounded, since H_4 given by (2.24) becomes unbounded. Similarly both coefficients B_2^+ and B_2^- of the $\phi_m \cos t$ and $\phi_m \sin t$ boundaries become singular when $B_{(1,n)} = B_{(2,m)}$, because the function H_3 given by (2.23) becomes unbounded. This leads to the two questions: Precisely which pairs of values of frequencies α and β can lead to such singularities? and; how can one unfold these codimension-two resonance tongue interactions, allowing both η and B to vary?

3.1 Multiple timescale asymptotic expansion

In order to seek an answer these questions, we shall develop a general multiple timescale asymptotic expansion about a given pair of values (B_0, η_0). Suppose that $B_0 = B_{\alpha,n}$ is the root point in the (B, ε)-plane of a resonance tongue corresponding to motion with angular frequency α. We shall consider the possibility that at precisely (B_0, η_0) there is the root point of a second resonance tongue so that $B_0 = B_{\alpha,n} = B_{\beta,m}$ for $m \neq n$. For the time being we do not assume any relation between the half-integers α and β, except of course the relation between the eigenvalues

$$\eta_0 = \frac{\lambda_n}{\alpha^2} = \frac{\lambda_m}{\beta^2}. \tag{3.2}$$

Since we do not know *a priori* which time scales will lead to a distinguished limit for this problem we will consider all functions now to be functions of a heirachy of time scales $(t,\ \tau_1 = \delta t,\ \tau_2 = \delta^2 t,\ \ldots)$, and introduce the the following expansions:

$$\left.\begin{aligned} u(s) &= \delta u_1(s,t,\tau_1,\tau_2) + \delta^2 u_2(s,t,\tau_1,\tau_2) + \delta^3 u_3(s,t,\tau_1,\tau_2) + \cdots, \\ \eta &= \tfrac{\lambda_n}{\alpha^2} + \delta\eta_1 + \delta^2\eta_2 + \cdots, \\ B &= B_0 + \delta B_1 + \delta^2 B_2 + \cdots, \\ & \varepsilon = \delta\varepsilon_1, \quad \gamma = \delta\gamma_1. \end{aligned}\right\} \tag{3.3}$$

Here, for future use in Sect. 5 below, we have retained material damping γ at the same order $O(\delta)$ as the amplitude of excitation ε. By keeping the small parameter δ separate from ε we allow for the possibility of having non-zero damping at zero excitation; $\varepsilon_1 = 0$, $\gamma_1 \neq 0$.

When these series are substituted into (2.6)-(2.8) and the coefficients of the terms up to δ^3 are set to zero, the result is

$$\frac{\lambda_n}{\alpha^2}\frac{\partial^2 u_1}{\partial t^2} + \mathrm{M}_0 u_1 = 0, \tag{3.4}$$

$$\frac{\lambda_n}{\alpha^2}\frac{\partial^2 u_2}{\partial t^2} + \mathrm{M}_0 u_2 = \varepsilon_1\frac{\lambda_n}{\alpha^2}\cos t \mathrm{L}u_1 - \eta_1\frac{\partial^2 u_1}{\partial t^2} - \frac{2\lambda_n}{\alpha^2}\frac{\partial^2 u_1}{\partial t\partial\tau_1} - B_1 u_1^{IV} - \gamma_1\frac{\lambda_n}{\alpha^2}\frac{\partial u_1^{IV}}{\partial t}, \tag{3.5}$$

$$\begin{aligned} \frac{\lambda_n}{\alpha^2}\frac{\partial^2 u_3}{\partial t^2} + \mathrm{M}_0 u_3 = {} & \varepsilon_1\frac{\lambda_n}{\alpha^2}\cos t \mathrm{L}u_2 - \eta_1\frac{\partial^2 u_2}{\partial t^2} - \frac{2\lambda_n}{\alpha^2}\frac{\partial^2 u_2}{\partial t\partial\tau_1} - B_1 u_2^{IV} - \gamma_1\frac{\lambda_n}{\alpha^2}\frac{\partial u_2^{IV}}{\partial t} + \\ & \varepsilon_1\eta_1\cos t \mathrm{L}u_1 - \eta_2\frac{\partial^2 u_1}{\partial t^2} - 2\eta_1\frac{\partial^2 u_1}{\partial t\partial\tau_1} - \frac{2\lambda_n}{\alpha^2}\frac{\partial^2 u_1}{\partial t\partial\tau_2} - \\ & \frac{\lambda_n}{\alpha^2}\frac{\partial^2 u_1}{\partial\tau_1^2} - B_2 u_1^{IV} - \gamma_1\frac{\lambda_n}{\alpha^2}\frac{\partial u_1^{IV}}{\partial\tau_1} - \gamma_1\eta_1\frac{\partial u_1^{IV}}{\partial t}. \end{aligned} \tag{3.6}$$

Here the linear operator M_0 is M (defined in (2.7)) evaluated at $B = B_0$:

$$\mathrm{M}_0 u = B_0 u^{IV} + \mathrm{L}u, \quad \text{with} \quad \mathrm{L}u = [(1-s)u']',$$

and $u_1(s),\ u_2(s),\ u_3(s)$, are each subject to the boundary conditions (2.8).

Following assumptions (3.2) on coexistent resonances, we shall take the $O(\delta)$ solution to be

$$\begin{aligned} u_1 = {} & [f(\tau_1,\tau_2,\ldots)\cos\alpha t + g(\tau_1,\tau_2,\ldots)\sin\alpha t]\phi_n(s) \\ & + [d(\tau_1,\tau_2,\ldots)\cos\beta t + e(\tau_1,\tau_2,\ldots)\sin\beta t]\phi_m(s). \end{aligned} \tag{3.7}$$

The functions f, g, e, d will be determined at higher-order by non-resonance conditions.

3.1.1 The $O(\delta^2)$ equation

Substituting the form (3.7) into the left-hand side of the $O(\delta^2)$ equation (3.5), we obtain

$$\begin{aligned}
&\frac{\lambda_n}{\alpha^2}\frac{\partial^2 u_2}{\partial t^2} + \mathrm{M}_0 u_2 = \\
&\quad \varepsilon_1 \frac{\lambda_n}{2\alpha^2}\mathrm{L}\phi_n \{f[\cos(\alpha+1)t + \cos(\alpha-1)t] + g[\sin(\alpha+1)t + \sin(\alpha-1)t]\} \\
&\quad + \left\{\eta_1\alpha^2\phi_n f - \frac{2\lambda_n}{\alpha}\frac{\partial g}{\partial \tau_1}\phi_n - B_1\phi_n^{IV} f - \gamma_1\frac{\lambda_n}{\alpha}\phi_n^{IV} g\right\}\cos\alpha t \\
&\quad + \left\{\eta_1\alpha^2\phi_n g + \frac{2\lambda_n}{\alpha}\frac{\partial f}{\partial \tau_1}\phi_n - B_1\phi_n^{IV} g + \gamma_1\frac{\lambda_n}{\alpha}\phi_n^{IV} f\right\}\sin\alpha t \\
&\quad + \quad \text{similar expressions with } \alpha \mapsto \beta, \quad (f,g) \mapsto (d,e), \quad n \mapsto m. \qquad (3.8)
\end{aligned}$$

The particular integral for u_2 can in general be expressed as

$$\begin{aligned}
u_2 = {} & H_1\cos\alpha t + H_2\sin\alpha t + F_1\cos\beta t + F_2\sin\beta t \\
& + H_3[f\cos(\alpha+1)t + g\sin(\alpha+1)t] + H_4[f\cos(\alpha-1)t + g\sin(\alpha-1)t] \\
& + F_3[d\cos(\beta+1)t + e\sin(\beta+1)t] + F_4[d\cos(\beta-1)t + e\sin(\beta-1)t], \qquad (3.9)
\end{aligned}$$

where

$$M_0H_1 - \lambda_n H_1 = \left(\eta_1\alpha^2\phi_n - B_1\phi_n^{IV}\right) f - \frac{2\lambda_n}{\alpha}\phi_n\frac{\partial g}{\partial\tau_1} - \gamma_1\frac{\lambda_n}{\alpha}\phi_n g, \qquad (3.10)$$

$$M_0H_2 - \lambda_n H_2 = \left(\eta_1\alpha^2\phi_n - B_1\phi_n^{IV}\right) g + \frac{2\lambda_n}{\alpha}\phi_n\frac{\partial f}{\partial\tau_1} + \gamma_1\frac{\lambda_n}{\alpha}\phi_n f, \qquad (3.11)$$

$$M_0H_3 - \frac{\lambda_n(\alpha+1)^2}{\alpha^2}H_3 = \varepsilon_1\frac{\lambda_n}{2\alpha^2}\mathrm{L}\phi_n, \qquad (3.12)$$

$$M_0H_4 - \frac{\lambda_n(\alpha-1)^2}{\alpha^2}H_4 = \varepsilon_1\frac{\lambda_n}{2\alpha^2}\mathrm{L}\phi_n, \qquad (3.13)$$

$$M_0F_1 - \lambda_m F_1 = \left(\eta_1\beta^2\phi_m - B_1\phi_m^{IV}\right) d - \frac{2\lambda_m}{\beta}\phi_m\frac{\partial e}{\partial\tau_1} - \gamma_1\frac{\lambda_m}{\beta}\phi_m e, \qquad (3.14)$$

$$M_0F_2 - \lambda_m F_2 = \left(\eta_1\alpha^2\phi_m - B_1\phi_m^{IV}\right) e + \frac{2\lambda_m}{\beta}\phi_m\frac{\partial d}{\partial\tau_1} + \gamma_1\frac{\lambda_m}{\beta}\phi_m d, \qquad (3.15)$$

$$M_0F_3 - \frac{\lambda_n(\beta+1)^2}{\alpha^2}F_3 = \varepsilon_1\frac{\lambda_n}{2\alpha^2}\mathrm{L}\phi_m, \qquad (3.16)$$

$$M_0F_4 - \frac{\lambda_n(\beta-1)^2}{\alpha^2}F_4 = \varepsilon_1\frac{\lambda_n}{2\alpha^2}\mathrm{L}\phi_m. \qquad (3.17)$$

In this section and the next we are interested in the zero-damping case, and so we now set

$$\gamma_1 = 0, \quad \varepsilon_1 = 1, \qquad \text{hence} \quad \delta \equiv \varepsilon,$$

and we shall use ε rather than δ as our expansion parameter.

3.1.2 Trivial solution at $O(\varepsilon^2)$

Let us assume for now that $\alpha, \beta \neq 1/2$. (The case $\alpha = 1/2$ leads to the fact that the $\sin(\alpha-1)t$ and $\cos(\alpha-1)t$ terms are included in the equations for the $\sin\alpha t$ and $\cos\alpha t$ coefficients so that the function H_4 is combined with functions H_1 and H_2). The solvability condition then gives the linear terms in $B_1^{\pm}$ given by (2.20). So, assuming

$$\alpha, \beta \geq 1, \tag{3.18}$$

we find that eqs. (3.12) and (3.13) have unique bounded solutions. The solvability condition comes from demanding that the right-hand sides of (3.10) and (3.11) should be orthogonal to ϕ_n, and the right-hand sides of (3.14) and (3.15) orthogonal to ϕ_m, which are eigenfunctions of the respective left-hand side operators. Hence, using the orthonormality of ϕ_n and ϕ_m, we obtain

$$\frac{\partial g}{\partial \tau_1} - \left(\eta_1\alpha^2 - B_1\langle\phi_n'', \phi_n''\rangle\right)\frac{\alpha}{2\lambda_n} f = 0, \tag{3.19}$$

$$\frac{\partial f}{\partial \tau_1} + \left(\eta_1\alpha^2 - B_1\langle\phi_n'', \phi_n''\rangle\right)\frac{\alpha}{2\lambda_n} g = 0, \tag{3.20}$$

$$\frac{\partial e}{\partial \tau_1} - \left(\eta_1\beta^2 - B_1\langle\phi_m'', \phi_m''\right)\frac{\beta}{2\lambda_m} d = 0, \tag{3.21}$$

$$\frac{\partial d}{\partial \tau_1} + \left(\eta_1\beta^2 - B_1\langle\phi_m'', \phi_m''\right)\frac{\beta}{2\lambda_m} e = 0. \tag{3.22}$$

These four equations can be simplified to read that f and g must both satisfy the equation

$$\frac{\partial^2 f}{\partial \tau_1^2} = -K_\alpha^2 f, \tag{3.23}$$

and both d and e satisfy

$$\frac{\partial^2 e}{\partial \tau_1^2} = -K_\beta^2 e, \tag{3.24}$$

where

$$K_\alpha = \left(\eta_1\alpha^2 - B_1\langle\phi_n'', \phi_n''\rangle\right)\frac{\alpha}{2\lambda_n}, \qquad K_\beta = \left(\eta_1\beta^2 - B_1\langle\phi_m'', \phi_m''\rangle\right)\frac{\beta}{2\lambda_m}. \tag{3.25}$$

We are looking for stability boundaries. That is where the functions f, g, d or e have neutrally stable solutions. Thinking of η as fixed, we find from (3.23)–(3.24) that this

happens for an isolated B_1-value for each of the equations (3.23) and (3.24), given by $K_\alpha = 0$ and $K_\beta = 0$ respectively. For all other values of B_1 the zero solution is a stable equilibrium. The two isolated values of B_1 are

$$B_1 = \frac{\eta_1 \alpha^2}{\langle \phi_n'', \phi_n'' \rangle}, \quad \text{or} \quad \frac{\eta_1 \beta^2}{\langle \phi_n'', \phi_m'' \rangle} \tag{3.26}$$

However, note that these two conditions (3.26) can be written more simply as

$$\sigma_1 = B_1 \langle \phi_p'', \phi_p'' \rangle \quad \text{where} \quad \lambda = \lambda_p + \varepsilon \sigma_1,$$

for $p = n$ or m. We recognize immediately that this is the first-order-in-ε correction to the curve (2.16) for the eigenvalues as a function of B if we demand that either the condition $\lambda = \eta\alpha^2$ or $\lambda = \eta\beta^2$ remains true at nearby (B, η)-values. In other words this moves the underlying B and η values to new ones that satisfy the appropriate eigenvalue condition (either of the two equalities in (3.2)). Since we are interested in expanding about η_0 and B_0, we must therefore choose

$$\eta_1 = B_1 = 0. \tag{3.27}$$

Equations (3.16) and (3.17) have a unique bounded solution unless $(\beta \pm 1)^2 = \alpha^2$. That is, unless

$$\beta = \alpha \pm 1. \tag{3.28}$$

If (3.28) is satisfied then the above asymptotic expansion becomes invalid and we note that the function F_3 or F_4 must be combined with H_1 or H_2 respectively. Then the non-resonance conditions (3.19) and (3.20) lead to non-trivial expressions for B_1 as a function of η_1. We shall treat these on a case by case basis in Secs. 3.3, 3.4 and 4 below. For the time being let us continue by assuming that (3.28) is *not* satisfied.

3.1.3 The $O(\varepsilon^3)$ equation

Assuming that (3.18) holds and (3.28) is not satisfied, so that (3.27) holds, the $O(\varepsilon^2)$ solution to eq. (3.6) is given by (3.9) where f, g, d and e are all independent of τ_1. Substitution of this form for u_2 into (3.6) yields

$$\begin{aligned}\frac{\lambda_n}{\alpha^2}\frac{\partial^2 u_3}{\partial t^2} + \mathrm{M}_0 u_3 = {} & \cos(\alpha-2)t \frac{\lambda_n}{2\alpha^2}\mathrm{L}H_4 f + \sin(\alpha-2)t\frac{\lambda_n}{2\alpha^2}\mathrm{L}H_4 g \\ & + \cos(\alpha-1)t\left\{\frac{\lambda_n}{2\alpha^2}\mathrm{L}H_1 f + \eta_1(\alpha_1-1)^2 H_4 f - B_1 H_4^{IV} f + \frac{1}{2}\eta_2 \mathrm{L}\phi_n f\right\}\end{aligned}$$

$$
\begin{aligned}
&+\sin(\alpha-1)t\left\{\frac{\lambda_n}{2\alpha^2}\mathrm{L}H_2g+\eta_1(\alpha-1)^2H_4g-B_1H_4^{IV}g+\frac{1}{2}\eta_2\mathrm{L}\phi_ng\right\}\\
&+\cos\alpha t\left\{\frac{\lambda_n}{2\alpha^2}(\mathrm{L}H_3+\mathrm{L}H_4)f+\eta_1\alpha^2H_1f-B_1H_1^{IV}\right.\\
&\left.+\,\eta_2\alpha^2\phi_nf-2\frac{\lambda_n}{\alpha}\phi_n\frac{\partial g}{\partial\tau_2}-B_2\phi_n^{IV}f\right\}\\
&+\sin\alpha t\left\{\frac{\lambda_n}{2\alpha^2}(\mathrm{L}H_3g+\mathrm{L}H_4g)+\eta_1\alpha^2H_2g-B_1H_2^{IV}g++\eta_2\alpha^2\phi_ng\right.\\
&\left.+\frac{2\lambda_n}{\alpha}\phi_n\frac{\partial f}{\partial\tau_2}-B_2\phi_n^{IV}g\right\}\\
&+\cos(\alpha+1)t\left\{\frac{\lambda_n}{2\alpha^2}\mathrm{L}H_1f+\eta_1(\alpha+1)^2H_3f-B_1H_3^{IV}f+\frac{1}{2}\eta_2\mathrm{L}\phi_nf\right\}\\
&+\sin(\alpha+1)t\left\{\frac{\lambda_n}{2\alpha^2}\mathrm{L}H_2g+\eta_1(\alpha+1)^2H_3g-B_1H_3^{IV}g+\frac{1}{2}\eta_2\mathrm{L}\phi_ng\right\}\\
&+\cos(\alpha+2)t\frac{\lambda_n}{2\alpha^2}\mathrm{L}H_3f\ +\sin(\alpha+2)t\frac{\lambda_n}{2\alpha^2}\mathrm{L}H_3g
\end{aligned}
\tag{3.29}
$$

$+$ similar expressions with $\alpha\mapsto\beta$, $(f,g)\mapsto(d,e)$, $n\mapsto m$ and $H_i\mapsto F_i$.

Let us now proceed to analyse the solution to the above equation in various special cases.

3.2 Codimension-one resonance; derivation of (2.17)

In order to obtain the 'linearised' results from Parts I and II, valid for undistinguished values of η, we drop all of the β terms in the above and set $\lambda_n/\alpha=\eta$. This describes the asymptotics of resonance tongues away from their codimension-two interactions. Furthermore we set set $\eta=\lambda_n/\alpha^2$, i.e. $\eta_1=\eta_2=\ldots 0$. Failure to do this will result in the corrections (2.16) for the η-values that define the resonance condition as B_0 varies. From (3.27) we have, provided $\alpha\neq 1/2$, that $B_1=0$. Consider now the α-dependent terms of (3.29). The solvability condition at this level is that the coefficients of $\cos\alpha t$ and $\sin\alpha t$ must be orthogonal to the eigenfunction ϕ_n. Now, provided that we do *not* satisfy

$$
\alpha\pm 1=\pm\alpha,\quad\text{or}\quad\alpha\pm 2=\pm\alpha,\qquad i.e.\quad\alpha=\frac{1}{2}\text{ or }1,
\tag{3.30}
$$

this leads to the conditions (making use of (2.10) (2.11))

$$
\frac{\partial f}{\partial\tau_2}=\left[\frac{B_2\alpha}{2\lambda_n}\langle\phi_n'',\phi_n''\rangle-\frac{1}{4\alpha}\left(\langle\phi_n,\mathrm{L}H_3\rangle+\langle\phi_n,\mathrm{L}H_4\rangle\right)\right]g
\tag{3.31}
$$

$$
\frac{\partial g}{\partial\tau_2}=-\left[\frac{B_2\alpha}{2\lambda_n}\langle\phi_n'',\phi_n''\rangle-\frac{1}{4\alpha}\left(\langle\phi_n,\mathrm{L}H_3\rangle+\langle\phi_n,\mathrm{L}H_4\rangle\right)\right]f.
\tag{3.32}
$$

Like (3.19) and (3.20), these equations can be expressed more simply by saying that both f and g satisfy

$$\frac{\partial f^2}{\partial \tau^2} = -K^2 f, \quad \text{where} \quad K = \frac{B_2 \alpha}{2\lambda_n} \langle \phi_n'', \phi_n'' \rangle - \frac{1}{4\alpha} \left(\langle \phi_n, \mathrm{L}H_3 \rangle + \langle \phi_n, \mathrm{L}H_4 \rangle \right).$$

Hence solutions are bounded, apart from at the single neutral stability point $K = 0$ given by

$$B_2 = \frac{\lambda_n}{2\alpha^2} \frac{\langle \phi_n, \mathrm{L}H_3 \rangle + \langle \phi_n, \mathrm{L}H_4 \rangle}{\langle \phi_n'', \phi_n'' \rangle}. \tag{3.33}$$

This shows that the width of the resonance tongue is not resolved at this level, but both boundaries of the tongue have the same quadratic coefficient $B_2 \varepsilon^2$ given by (3.33).

Now suppose that one of (3.30) *is* satisfied. Consider first $\alpha = 1/2$, which case we have already shown leads to a non-trivial width of resonance tongue at $O(\varepsilon)$; $B = B_0 + \varepsilon B_1^{\pm} + O(\varepsilon^2)$. From the $O(\varepsilon^3)$ equation (3.29), we see that the coefficient of $\cos(\alpha - 1)t$ must be added to those of $\cos \alpha t$ when seeking the orthogonality condition, and similarly the coefficient of $\sin(\alpha - 1)t$ must be *subtracted* from that of $\sin \alpha t$. This will lead to different equations for B_2 and separate non-trivial corrections to the two boundaries of the resonance tongue $B = B_0 + \varepsilon B_1^{\pm} + \varepsilon^2 B_2^{\pm} + O(\varepsilon^3)$.

Consider now $\alpha = 1$. Here the coefficient of $\cos(\alpha - 2)t$ in (3.29) must be added to that of $\cos \alpha t$ when seeking the orthogonality condition, and similarly the coefficient of $\sin(\alpha - 2)t$ must be *subtracted* from that of $\sin \alpha t$. This will lead to different equations for B_2 and separate non-trivial corrections to the two boundaries corresponding to $\cos \alpha t$ and $\sin \alpha t$. In fact, it is easy to see that we get $B = B_0 + \varepsilon^2 B_2^{\pm}$, where $B_2^{\pm}$ are given by (2.21), (2.22) with $\eta = \lambda_n$.

Returning to the general case $\alpha \neq 1/2$ or 1, suppose we carry out the expansion to $O(\varepsilon^4)$. We would then get contributions to the particular integral u_4 from terms which come from the expansion of

$$\left\{ \begin{array}{c} \cos \\ \sin \end{array} \right\} (\alpha \pm 1)t \cdot \cos t, \quad \text{and} \quad \left\{ \begin{array}{c} \cos \\ \sin \end{array} \right\} (\alpha \pm 2)t \cdot \cos t,$$

which we lead to terms proportional to

$$\left\{ \begin{array}{c} \cos \\ \sin \end{array} \right\} (\alpha \pm 3)t.$$

Therefore, provided we do *not* satisfy

$$\alpha \pm 3 = \pm \alpha, \quad \textit{i.e.} \quad \alpha = 3/2 \quad (\text{since } \alpha > 0),$$

then the orthogonality condition applied to the $\sin\alpha t$ and $\cos\alpha t$ equations leads to a unique condition for B_3, which is third-order correction to both resonance tongues $B = B_0 + \varepsilon^2 B_2 + \varepsilon^3 B_3$. If, however, $\alpha = 3/2$ then we get a different contribution from the $\sin(\alpha-3)t$, and $\cos(\alpha-3)t$ terms, leading to non-equal corrections $B_3^{\pm}$. as was Hence the first non-trivial width of the resonance tongue is $O(\varepsilon^3)$.

Extrapolating this argument we see that the first non-trivial width of any resonance tongue is always at $O(\varepsilon^{2\alpha})$, and we recover the general expression (2.17). The asymptotic procedure we have developed can in principle calculate all the coefficients B_j, $j = 2, \ldots, 2\alpha-1$, and $B_{2\alpha}^{\pm}$ for any arbitrary half-integer α, but the expressions become rather cumbersome beyond $O(\varepsilon^3)$.

3.3 Resonance interaction at $O(\varepsilon^2)$

Now let us reintroduce β and assume that $\eta = (\lambda_n/\alpha^2) + \varepsilon\eta_1 + \varepsilon^2\eta_2 + \ldots$. Consider what happens at $O(\varepsilon^2)$ when (3.28) is satisfied, which without loss of generality we assume occurs with

$$\beta = \alpha + 1 \tag{3.34}$$

(avoiding for the time being the special cases $\alpha = 0$ or $\alpha = 1/2$). As we already remarked, the asymptotic expansion we have introduced above becomes invalid when (3.34) is satisfied. In particular we can no longer assume $B_1 = \eta_1 = 0$. If we do so then we reach the contradiction that eq. (3.17) has a solution that is an eigenfunction, but the right-hand side is not orthogonal to ϕ_m. Instead we must combine F_4 (which is the coefficient of $d\cos(\beta-1)t$ and $e\sin(\beta-1)t$ into the functions H_1 and H_2 via

$$\tilde{H}_1 = H_1 + F_4, \quad \tilde{H}_2 = H_2 + F_4.$$

Then $\tilde{H}_1$ and $\tilde{H}_2$ satisfy

$$M_0\tilde{H}_1 - \lambda_n\tilde{H}_1 = \eta_1\alpha^2\phi_n f - B_1\phi_n^{IV} f + \frac{\lambda_n}{2\alpha^2}\mathrm{L}\phi_m d - \frac{\partial g}{\partial\tau_1}\left(\frac{2\lambda_n}{\alpha}\phi_n\right), \tag{3.35}$$

$$M_0\tilde{H}_2 - \lambda_n\tilde{H}_2 = \eta_1\alpha^2\phi_n g - B_1\phi_n^{IV} g + \frac{\lambda_n}{2\alpha^2}\mathrm{L}\phi_m e + \frac{\partial f}{\partial\tau_1}\left(\frac{2\lambda_n}{\alpha}\phi_n\right). \tag{3.36}$$

Similarly, the term H_3 proportional to $f\cos(\alpha+1)t$ and $g\sin(\alpha+1)t$ must be added to the functions F_1 and F_2 via

$$\tilde{F}_1 = F_1 + H_3, \quad \tilde{F}_2 = F_2 + H_3,$$

where $\tilde{F}_1$ and $\tilde{F}_2$ satisfy

$$M_0\tilde{F}_1 - \lambda_m\tilde{F}_1 = \eta_1\beta^2\phi_m d - B_1\phi_m^{IV}d + \frac{\lambda_m}{2\beta^2}\mathrm{L}\phi_n f - \frac{\partial e}{\partial\tau_1}\left(\frac{2\lambda_m}{\beta}\phi_m\right), \tag{3.37}$$

$$M_0\tilde{F}_2 - \lambda_m\tilde{F}_2 = \eta_1\alpha^2\phi_m e - B_1\phi_m^{IV}e + \frac{\lambda_m}{2\beta^2}\mathrm{L}\phi_n g + \frac{\partial d}{\partial\tau_1}\left(\frac{2\lambda_m}{\beta}\phi_m\right). \tag{3.38}$$

The solvability condition is now that the right-hand sides of (3.35) and (3.36) should both be orthogonal to ϕ_n and that the right-hand sides of (3.37) and (3.38) should be orthogonal to ϕ_m. This gives

$$\frac{\partial g}{\partial\tau_1} - \frac{\alpha}{2\lambda_n}\left(\eta_1\alpha^2 - B_1\langle\phi_n'',\phi_n''\rangle\right)f - \frac{1}{4\alpha}\langle\phi_n,\mathrm{L}\phi_m\rangle d = 0, \tag{3.39}$$

$$\frac{\partial f}{\partial\tau_1} + \frac{\alpha}{2\lambda_n}\left(\eta_1\alpha^2 - B_1\langle\phi_n'',\phi_n''\rangle\right)g + \frac{1}{4\alpha}\langle\phi_n,\mathrm{L}\phi_m\rangle e = 0, \tag{3.40}$$

$$\frac{\partial e}{\partial\tau_1} - \frac{(\alpha+1)}{2\lambda_m}\left(\eta_1(\alpha+1)^2 - B_1\langle\phi_m'',\phi_m''\rangle\right)d - \frac{1}{4(\alpha+1)}\langle\phi_n,\mathrm{L}\phi_m\rangle f = 0, \tag{3.41}$$

$$\frac{\partial d}{\partial\tau_1} + \frac{(\alpha+1)}{2\lambda_m}\left(\eta_1(\alpha+1)^2 - B_1\langle\phi_m'',\phi_m''\rangle\right)e + \frac{1}{4(\alpha+1)}\langle\phi_n,\mathrm{L}\phi_m\rangle g = 0. \tag{3.42}$$

From the form of these equations we note that the they are expressible as a system

$$\frac{\partial x}{\partial\tau_1} = A(x), \qquad \text{where} \quad x = \begin{bmatrix} f \\ d \\ g \\ e \end{bmatrix}, \quad A = \begin{bmatrix} 0 & 0 & -a_1 & -a_2 \\ 0 & 0 & -a_3 & -a_4 \\ a_1 & a_2 & 0 & 0 \\ a_3 & a_4 & 0 & 0 \end{bmatrix},$$

with

$$a_1 = \frac{\alpha}{2\lambda_n}\left(\eta_1\alpha^2 - B_1\langle\phi_n'',\phi_n''\rangle\right), \qquad a_2 = \frac{1}{4\alpha}\langle L\phi_m,\phi_n\rangle,$$

$$a_3 = \frac{1}{4(\alpha+1)}\langle L\phi_m,\phi_n\rangle, \qquad a_4 = \frac{(\alpha+1)}{2\lambda_m}\left(\eta_1(\alpha+1)^2 - B_1\langle\phi_m'',\phi_m''\rangle\right). \tag{3.43}$$

From the form of A we conclude that its eigenvalues are all double and pure imaginary unless

$$a_1a_4 - a_2a_3 = 0. \tag{3.44}$$

Hence the zero solution to the system (3.39)–(3.42) is stable unless we sit precisely on this neutral stability curve defined by (3.44). The fact that all eigenvalues of A are then zero implies that (3.44) is the neutral stability condition for both the cosine mode (corresponding to coefficients f and d) and the sine mode (with coefficients g and e). Hence at this $O(\varepsilon)$ level the resonance tongue has zero width.

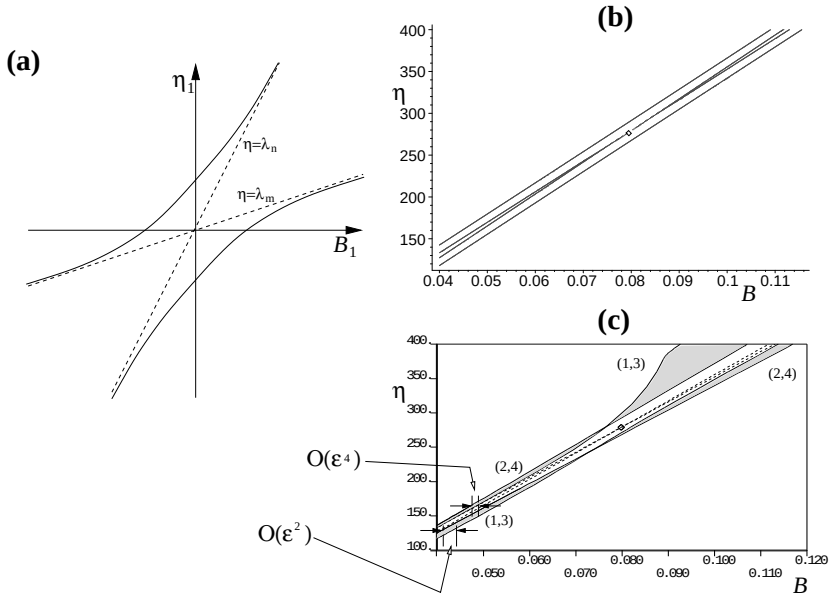

Figure 4: (a) Schematic diagram of the interaction at $O(\varepsilon)$ of the resonance tongues corresponding to α and $\beta = \alpha + 1$ according to eq. (3.45). The dashed lines represent the eigenvalue loci $B_{\alpha,n}(\eta)$ and $B_{\beta,m}(\eta)$ and the solid line gives the $O(\varepsilon)$ correction. Note that at this order both tongues have zero width, provided $\alpha \geq 1$. (b),(c) Numerical illustration in the case $(\alpha, n) = (1, 3)$, $(\beta, m) = (2, 4)$ and $\varepsilon = 0.02$. Panel (b) shows the evaluation of the formula (3.45) (outer two curves) together with the eigenvalue loci $B = B_{1,3}(\eta)$ and $B = B_{2,4}(\eta)$ which cross at $\eta = 278.808$ (marked by a diamond). Panel (c) shows the numerically computed stability boundaries using Floquet theory with $N = 4$. The eigenvalue loci are dashed. Shaded regions correspond to instability inside the resonance tongue.

It remains to express the neutral stability condition as a curve in the (B_1, η_1)-plane. Substitution of (3.43) into (3.44) results in

$$\Big(\eta_1\alpha^2 - B_1\langle\phi_n'', \phi_n''\rangle\Big)\Big(\eta_1(\alpha+1)^2 - B_1\langle\phi_m'', \phi_m''\rangle\Big) = \frac{\lambda_n^2}{4\alpha^4}\langle\phi_m, L\phi_n\rangle^2, \tag{3.45}$$

where we have used $\lambda_m = \lambda_n(\alpha+1)^2/\alpha^2$. Note that the right-hand side of (3.45) is strictly positive, whereas the left-hand side is the product of two linear functions of η_1 and B_1.

This is the equation for a hyperbola in the (η_1, B_1)-plane, see Fig. 4(a). In the limit that $|\eta_1|$ is large, the locus of solutions becomes two straight lines with slopes $\frac{1}{\alpha^2}\langle\phi_n'', \phi_n''\rangle$ and $\frac{1}{(\alpha+1)^2}\langle\phi_m'', \phi_m''\rangle$ which according to (2.16) are precisely the linear approximations to the loci $B_{\alpha,n}(\eta)$ and $B_{\alpha+1,m}(\eta)$. Hence a long way from the resonance tongue interaction there

is no correction at $O(\varepsilon)$ to the root points of the resonance tongues (as expected from the results of the previous subsection). Note however, as shown in Fig. 4 the solution at finite values of the excitation ε that was attached to the (α, n) tongue for $\eta_1 \ll 0$ switches over to become associated with the $(\alpha+1, m)$ tongue for $\eta_1 \gg 0$.

Figure 4 numerically illustrates a particular resonance tongue interaction between the tongues $(1,3)$ and $(2,4)$. Note from Fig. 3 that these two resonance tongues switch their order (the relative B-values for which they occur) between $\eta = 120$ and $\eta = 360$. In fact we find numerically that these two resonances interact at

$$\eta_0 = 278.809, \quad B_0 = 0.0798242,$$

from which we have calculated that

$$\langle \phi_3'', \phi_3'' \rangle = 3807.75, \quad \langle \phi_4'', \phi_4'' \rangle = 14618.8, \quad \langle \phi_4'', \mathrm{L}\phi_3'' \rangle = 8.55440.$$

Using these quantities, the loci of the $O(\varepsilon)$ behaviour of the tongues, (3.45) is calculated and plotted in Fig. 4(b). Note that the slopes of the loci $\eta = B_{1,3}$ and $\eta = B_{2,4}$ are much closer than in the schematic panel (a). Finally, panel (c) of the figure shows how these results compare with a full numerical evaluation of the resonance tongues using Floquet theory for fixed amplitude $\varepsilon = 0.02$. Note that the tongues, which are $O(\varepsilon^2)$ and $O(\varepsilon^4)$ in theory away from the interaction (marked at the left-hand edge of the figure) undergo an abrupt change as they pass through a neighbourhood of the resonance tongue interaction point. There are several features to this change. First, as predicted and in broad quantitative agreement with the results in panel (b), the resonance tongues do not cross, but each tongue becomes attached to the opposite instability. Second, there is a point close to the codimension-two point at which each tongue (at this value of ε) 'pinches off'. The result is that the cosine and sine boundaries switch sides. This pinching off of the resonance tongue is not part of the above $O(\varepsilon)$ theory, but can be seen here as a necessary consequence of the resonance tongue interaction process. Note that such pinching of resonance tongues has been described before for one-degree of freedom parametrically excited systems (Broer & Levi 1995). (It is also in evidence in Fig. 3 where for $\eta = 360$, both the (1,3) and (2,4) resonance tongues become narrower for ε-values towards the top of the graph, suggesting that they pinch off for higher ε still (indeed they do); also the tongue (2,5) can be seen to undergo just such a pinching at $\varepsilon \approx 0.035$.) Finally, note that beyond the codimension-two point the $(1,3)$ tongue suddenly becomes much fatter. This is because of its interaction with the buckling mode instability at $B = B_{0,1} = 0.127594$ which was discussed in Part II, sect. 4(e), and will be treated further in Sect. 4 below.

3.4 The case $\alpha = 1/2, \beta = 3/2$; singularity in the sub-harmonic resonance

This case is special because the $O(\varepsilon)$ correction due to the resonance tongue interaction is at the same order as the $O(\varepsilon)$ width of the resonance tongue itself. Proceeding as in Sect. 3.3 above, we find that the term $H_3 f \cos(\alpha+1)$ in (3.9) must be added to $\tilde{H}_1$, and the term $H_3 g \sin(\alpha+1)$ subtracted from $\tilde{F}_1$. Hence the solvability condition becomes

$$\frac{\partial g}{\partial \tau_1} - \left(\frac{\eta_1}{16\lambda_n} - \frac{B_1\langle\phi_n'',\phi_n''\rangle}{4\lambda_n} + \frac{\langle\phi_n, L\phi_n\rangle}{2}\right) f - \frac{\langle L\phi_m,\phi_n\rangle}{2} d = 0 \qquad (3.46)$$

$$\frac{\partial f}{\partial \tau_1} + \left(\frac{\eta_1}{16\lambda_n} - \frac{B_1\langle\phi_n'',\phi_n''\rangle}{4\lambda_n} - \frac{\langle\phi_n, L\phi_n\rangle}{2}\right) g + \frac{\langle L\phi_m,\phi_n\rangle}{2} e = 0 \qquad (3.47)$$

$$\frac{\partial e}{\partial \tau_1} - \left(\frac{9\eta_1}{48\lambda_n} - \frac{B_1\langle\phi_m'',\phi_m''\rangle}{12\lambda_n}\right) d - \frac{\langle L\phi_m,\phi_n\rangle}{6} f = 0 \qquad (3.48)$$

$$\frac{\partial d}{\partial \tau_1} + \left(\frac{9\eta_1}{48\lambda_n} - \frac{B_1\langle\phi_n'',\phi_n''\rangle}{12\lambda_n}\right) e + \frac{\langle L\phi_m,\phi_n\rangle}{6} g = 0 \qquad (3.49)$$

The neutral mode solution of this equation can be written similarly to (3.44) in the form

$$9(a_1 \pm a_5)a_4 - a_2 a_3 = 0, \quad \text{where} \quad a_5 = \frac{\langle\phi_n, L\phi_n\rangle}{2}, \qquad (3.50)$$

$a_1, \ldots a_4$ are given by (3.43), and the sign '+' corresponds to the cosine mode and '−' to the sine mode.

Expanding (3.50) we obtain the pair of loci in the (B_1, η_1)-plane

$$\left(\frac{\eta_1}{4} - B_1\langle\phi_n'',\phi_n''\rangle \pm 2\lambda_n\langle\phi_n, L\phi_n\rangle\right)\left(\frac{9\eta_1}{4} - B_1\langle\phi_m'',\phi_m''\rangle\right) = \frac{4}{9}\lambda_n^2\langle\phi_m, L\phi_n\rangle^2. \qquad (3.51)$$

These loci describe the two hyperbolae which bound the shaded region shown schematically in Fig. 5(a), that asymptote for large η_1 and B_1 to the straight lines

$$B_1 = B_{n,1/2} \pm B_1^{\pm} = \frac{\eta_1}{4\langle\phi_n'',\phi_n''\rangle} \pm \frac{\langle\phi_n, L\phi_n\rangle}{\langle\phi_n'',\phi_n''\rangle}, \quad \text{and} \quad B_1 = B_{m,3/2} = \frac{9\eta_1}{4\langle\phi_n'',\phi_n''\rangle} \qquad (3.52)$$

which are the $O(\varepsilon)$ expressions for the two stability boundaries in the absence of their interaction. The region of instabilities for a finite ε are shaded in Fig. 5(a), and are obtained by noting the inequalities that must be true in order for Eqns. (3.46)–(3.49) to have bounded solutions. The resonance conditions $B_1 = B_{n,1/2}$ and $B_{m,3/2}$, valid when $\varepsilon = 0$ are depicted as dashed lines in the figure. Observe that the interaction between the two instabilities causes a small region of *stability* for finite ε in a neighbourhood of the critical point $\eta_1 = B_1 = 0$ where the two resonance curves $B_{n,1/2}$ and $B_{m,3/2}$ cross.

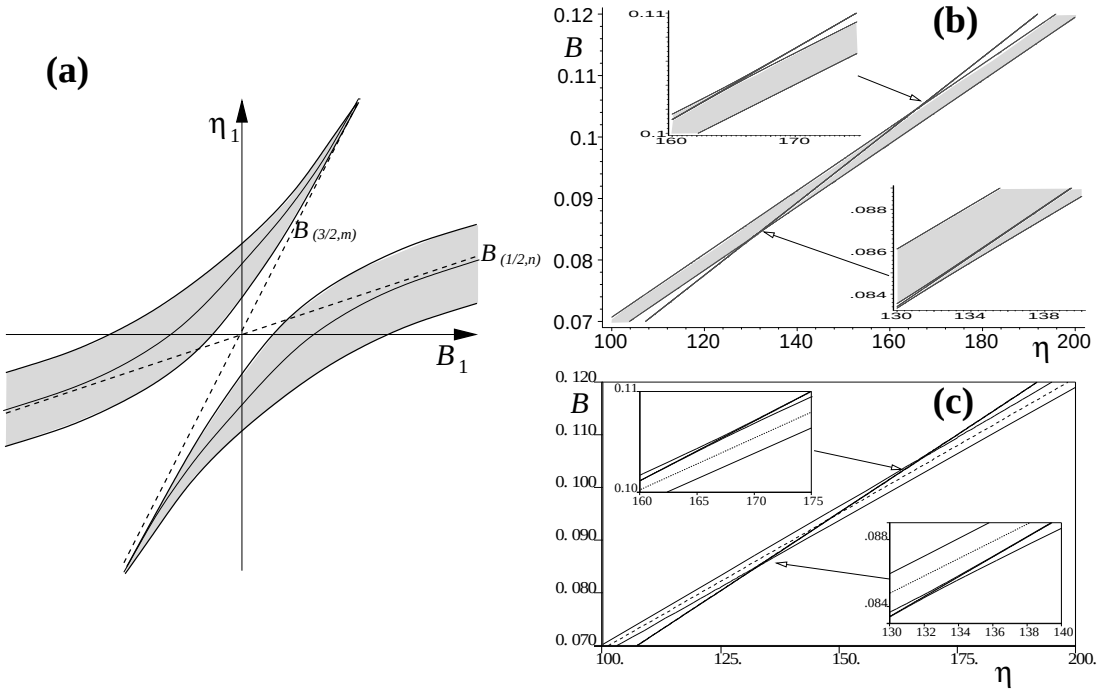

Figure 5: The interaction at $O(\varepsilon)$ of the resonance tongues corresponding to $\alpha = 1/2$ and $\beta = 3/2$. (a) Schematic picture; the shaded region corresponds to that of instability. (b) Evaluation of the formula (3.51) for $n = 2$, $m = 3$, using numerically calculated eigenfunctions ϕ_n and ϕ_m and $\varepsilon = 0.001$. (c) Numerically computed stability boundaries using Floquet theory with $N = 4$. The dashed line, like in part (a), corresponds to the locus $B = B_{1/2,2}(\eta)$. The locus $B = B_{3/2,3}$ is indistinguishable in this plot from the corresponding tongue boundary with finite ε.

By numerical computation we have found numerous examples of resonance tongue interaction of this kind. For example, taking $n = 2$ and $m = 3$ we find that $\lambda_n = \eta/4$ and $\lambda_m = 9\eta/4$ at $(B, \eta) = (0.0941064, 148.084)$. Note that this B-value is a little less than $B_c = 0.127594$ which implies that this interaction of instabilities is occuring for rods which are already marginally unstable to self-weight buckling. At those parameter values, computation of the eigenfunctions reveals

$$\langle \phi_n'', \phi_n'' \rangle = 485.765, \quad \langle \phi_m'', \phi_m'' \rangle = 3807.41, \quad \langle \phi_n, \mathrm{L}\phi_n \rangle = -8.69181, \quad \langle \phi_m, \mathrm{L}\phi_n \rangle = -1.946423. \tag{3.53}$$

Using these precise values, Fig. 5(b) shows the evaluation of the loci (3.51) with $\varepsilon = 0.001$, which are compared in Fig. 5(c) to the computation of the same stability boundaries using the numerical Floquet theory introduced in Part *I*. Note from the values (3.53) that the the straight lines $B_{1/2,2}$ and $B_{3/2,3}$ given by (3.52) with $n = 2$ and $m = 3$ have slopes that differ by less than 10%. Hence the stability region caused by the interaction between these two resonances is very small compared to the width of the instability tongues around $B = B_{1/2,2}$ (see insets).

3.5 Resonance interaction at higher order

The above analysis can be continued to $O(\varepsilon^3)$ to obtain the $O(\varepsilon^2)$ corrections to the four solid lines in Fig. 5(a). Carrying out the expansion to $O(\varepsilon^4)$ would show how to couple the shapes of the shaded instability boundaries to the $O(\varepsilon^3)$-thick resonance tongue around the locus $B = B_{m,3/2}$ which itself would be a curved with non-zero coefficient of ε^2 and ε^3. There is little extra qualitative information to be obtained by carrying out these expansions explicitly. Instead, let us focus on other resonance-tongue interactions which can only be captured by going to $O(\varepsilon^3)$ or higher.

Suppose first that (3.28) is not satisfied, but instead

$$\beta = \alpha \pm 2, \quad \text{without loss of generality} \quad \beta = \alpha + 2$$

The analysis at $O(\varepsilon^2)$ now proceeds as in Sec. 3.1.1 and we have $B_1 = \eta_1 = 0$. Consider the $O(\varepsilon^3)$ equation (3.29). Then the coefficients of $\cos(\beta - 2)t$ and $\sin(\beta - 2)t$ are also resonant and must be added to the coefficients of $\cos \alpha t$ and $\sin \alpha t$ to form solvability conditions. Also the coefficients of $\cos(\alpha + 2)t$ and $\sin(\alpha + 2)t$ should be added to those for $\cos \beta t$ and $\sin \beta t$. Again their will be two pairs of relations, from orthogonality to ϕ_n

and ϕ_m separately. This will lead to a non-trivial equation linking B_2 and η_2, like (3.45) for η_1 and B_1 in the case of a lower-order resonance tongue interaction.

So we find in general that the coefficient of ε^3 in the asymptotics of the resonance tongues undergoes a singularity which is patched up by this correction to the $O(\varepsilon^2)$ coefficient B_2 as η passes through η_0. Similarly, by extrapolation of the above argument to higher powers of ε in our asymptotic expansion, we find that if

$$\beta = \alpha + n$$

then there is a singularity in the $O(\varepsilon^{n+1})$ coefficient of the resonance tongues which is resolved by showing that there is a non-trivial contribution to the $O(\varepsilon^n)$ coefficient as η passes through the critical value at which the interaction occurs.

4 The case $\alpha = 1, \beta = 0$; first-harmonic buckling interaction

The case $\alpha = 1,\ \beta = 0$ leads to quite different results since instead of a resonance tongue, we have a single neutral stability curve corresponding to the rod 'falling over' into one of its buckling modes. The book-keeping in Sec. 3.3 above shows that this interaction causes a singularity in the $O(\varepsilon^2)$ coefficient B_2 of this instability curve in the (B, ε)-plane. Clearly this can have a profound effect on the stability analysis of the slightly longer than critical column, because it was precisely the negativity of this coefficient B_2 that gave the stabilization effect referred to colloquially as the 'Indian rope trick' in parts I and II.

Consider a neighbourhood of a special η-value $\eta = \lambda_n$ at which $B_{1,n} = B_{0,m}$. Particular physical interest is in the case $m = 1$, in which case we consider the column that is only slightly longer (or shorter) than the length of column that will just stand under it own weight. That is $B \approx B_c = B_{0,1}$, the critical value of the dimensionless parameter B for self-weight buckling. We shall denote the critical eigenmode corresponding to B_c as ϕ_c and the eigenmode corresponding to the pure dynamic instability ϕ_n. In fact, the analysis below works equally well for $B_c = B_{0,m}$ for any $m \geq 2$, except that 'stability' implies then 'stable to vibration mode m' rather than absolute stability since such a rod is statically unstable to modes ϕ_p, $p = 1, \ldots n-1$.

Thus the solution of the $O(\varepsilon)$ eq. (3.4) we take is

$$u_1 = \{h(\tau_1,\tau_2)\phi_c(s) + [f(\tau_1,\tau_2)\cos t + g(\tau_1,\tau_2)\sin t]\phi_n(s)\}\,, \tag{4.1}$$

with $\phi_m(s)$ and $\phi_c(s)$ subject to the boundary conditions (2.8).

4.1 The $O(\varepsilon^2)$ interaction equation

When the solution (4.1) is substituted into the right-hand side of the $O(\varepsilon^2)$ eq. (3.5) the result is

$$\begin{aligned}
&\lambda_n\frac{\partial^2 u_2}{\partial t^2} + \mathrm{M}_0 u_2 = \\
&\quad \frac{1}{2}\lambda_n\left[f(1+\cos 2t) + g\sin 2t\right]\mathrm{L}\phi_n - B_1 h\phi_c^{IV} + \\
&\quad \left[\left(\eta_1 f - 2\lambda_n\frac{\partial g}{\partial\tau_1}\right)\phi_n + \lambda_n h\mathrm{L}\phi_c - B_1 f\phi_n^{IV}\right]\cos t + \\
&\quad \left[\left(\eta_1 g + 2\lambda_n\frac{\partial f}{\partial\tau_1}\right)\phi_n - B_1 g\phi_n^{IV}\right]\sin t.
\end{aligned} \tag{4.2}$$

The particular integral of eq. (4.2) is

$$\begin{aligned}
u_2 \;=\; &\{H_0(s,\tau_1,\tau_2) + H_1(s,\tau_1,\tau_2)\cos t + H_2(s,\tau_1,\tau_2)\sin t + \\
&H_3(s)(f\cos 2t + g\sin 2t)\}
\end{aligned} \tag{4.3}$$

where

$$\mathrm{M}_0 H_0 \;=\; \frac{1}{2}\lambda_n f\mathrm{L}\phi_n - B_1 h\phi_c^{IV}, \tag{4.4}$$

$$\mathrm{M}_0 H_1 - \lambda_n H_1 \;=\; -\left(2\lambda_n\frac{\partial g}{\partial\tau_1} - \eta_1 f\right)\phi_n + \lambda_n h\mathrm{L}\phi_c - B_1 f\phi_n^{IV}, \tag{4.5}$$

$$\mathrm{M}_0 H_2 - \lambda_n H_2 \;=\; \left(2\lambda_n\frac{\partial f}{\partial\tau_1} + \eta_1 g\right)\phi_n - B_1 g\phi_n^{IV} \tag{4.6}$$

$$\mathrm{M}_0 H_3 - 4\lambda_n H_3 \;=\; \frac{1}{2}\lambda_n\mathrm{L}\phi_n, \tag{4.7}$$

and H_0, H_1 H_2 and H_3 must satisfy boundary conditions (2.8). Applying orthogonality with respect to ϕ_c to the right-hand side of eq. (4.4), we obtain

$$\frac{1}{2}\lambda_n\langle\phi_c, \mathrm{L}\phi_n\rangle f - B_1\langle\phi_c'', \phi_c''\rangle h = 0,$$

which, using (2.11), we can rewrite as

$$h = -\left(\frac{\lambda_n B_c \langle \phi_n'', \phi_c'' \rangle}{2B_1 \langle \phi_c'', \phi_c'' \rangle}\right) f := -\frac{G_n}{B_1} f. \tag{4.8}$$

Applying orthogonality with respect to ϕ_m to the right-hand sides of eqs. (4.5) and (4.6) yields

$$\frac{\partial g}{\partial \tau_1} - \left(\frac{\eta_1}{2\lambda_n} - \frac{B_1 \langle \phi_n'', \phi_n'' \rangle}{2\lambda_n} + \frac{\lambda_n B_c^2 \langle \phi_n'', \phi_c'' \rangle^2}{4B_1 \langle \phi_c'', \phi_c'' \rangle}\right) f = 0, \tag{4.9}$$

$$\frac{\partial f}{\partial \tau_1} + \left(\frac{\eta_1}{2\lambda_n} - \frac{B_1 \langle \phi_n'', \phi_n'' \rangle}{2\lambda_n}\right) g = 0. \tag{4.10}$$

Thus f and g both satisfy the differential equation

$$\frac{\partial^2 f}{\partial \tau_1^2} + \left(\frac{\eta_1}{2\lambda_n} - \frac{B_1 \langle \phi_n'', \phi_n'' \rangle}{2\lambda_n}\right)\left(\frac{\eta_1}{2\lambda_n} - \frac{B_1 \langle \phi_n'', \phi_n'' \rangle}{2\lambda_n} + \frac{\lambda_n B_c^2 \langle \phi_n'', \phi_c'' \rangle^2}{4B_1 \langle \phi_c'', \phi_c'' \rangle}\right) f = 0. \tag{4.11}$$

In order for this equation to have bounded sinusoidal solutions on timescale τ_1 we must have

$$\left(\frac{\eta_1}{2\lambda_n} - \frac{B_1 \langle \phi_n'', \phi_n'' \rangle}{2\lambda_n}\right)\left(\frac{\eta_1}{2\lambda_n} - \frac{B_1 \langle \phi_n'', \phi_n'' \rangle}{2\lambda_n} + \frac{\lambda_n B_c^2 \langle \phi_n'', \phi_c'' \rangle^2}{4B_1 \langle \phi_c'', \phi_c'' \rangle}\right) > 0, \tag{4.12}$$

and the stability boundaries in (η, B, ε)-space are determined by the zeros of the above expression.

One boundary is determined by

$$\left(\frac{\eta_1}{2\lambda_n} - \frac{B_1 \langle \phi_n'', \phi_n'' \rangle}{2\lambda_n}\right) := \sigma_1 = 0, \quad \text{hence} \quad \eta_1 = B_1 \langle \phi_n'', \phi_n'' \rangle. \tag{4.13}$$

In this case f is independent of τ_1 by eq. (4.10) and, unless $f \equiv 0$, g will be a linear function of τ_1 by eq. (4.9) and hence unbounded as $\tau_1 \to \infty$. Thus g is constant as a function of τ_1, which implies the motion is $\sin t$, out of phase with the drive.

The other boundary is determined by

$$\left(\frac{\eta_1}{2\lambda_n} - \frac{B_1 \langle \phi_n'', \phi_n'' \rangle}{2\lambda_n} + \frac{\lambda_n B_c^2 \langle \phi_n'', \phi_c'' \rangle^2}{4B_1 \langle \phi_c'', \phi_c'' \rangle}\right) := \sigma_2 = 0 \tag{4.14}$$

hence

$$\eta_1 = B_1 \langle \phi_n'', \phi_n'' \rangle - \frac{\lambda_n^2 B_c^2 \langle \phi_n'', \phi_c'' \rangle^2}{2B_1 \langle \phi_c'', \phi_c'' \rangle}$$

In this case g is independent of τ_1 by eq. (4.9) and therefore unless $g \equiv 0$, f will be a linear function of τ_1, and unbounded on this boundary. With this choice f and h are at most functions of τ_2, which implies a motion that is in phase with the drive, but with a non-zero lean (proportional to a constant plus $\cos t$).

To determine on which side of these boundaries solutions are stable we simply observe that for stability we must have $\sigma_1\sigma_2 > 0$ so that σ_1 and σ_2 must be either both negative or both positive. The regions of stability are shown as shaded in Fig. 6(a)

4.2 Correction at $O(\varepsilon^3)$

We now construct the correction $B_2\varepsilon^2$ and $\eta_2\varepsilon^2$ to these stability boundaries. This is necessary in order to see how the above $O(\varepsilon)$ correction matches the limit when the two resonances are a long way from interaction. In that case, both the falling over and harmonic instabilities are quadratic to leading order (formulae (2.18), (2.22) and (2.21)). We shall consider a neighbourhood of the boundaries $\sigma_1 = 0$ and $\sigma_2 = 0$ separately.

4.2.1 Case $\sigma_1 = 0$

As shown above, on this boundary $f \equiv 0$ so that $h \equiv 0$ by eq. (4.8), and $g = g(\tau_2)$. The right-hand-side of eqs. (4.4) and (4.5) are zero in this case so that H_0 and H_1 are proportional to ϕ_c and ϕ_n respectively. Thus, this part of the $O(\varepsilon^2)$ solution can be absorbed into the $O(\varepsilon)$, solution, and without loss of generality we can set $H_0 = H_1 \equiv 0$. The solution (4.3) can now be written as

$$\left.\begin{aligned} u_1 &= \phi_n(s)\sin t\, g(\tau_2), \\ u_2 &= \{H_2(s)\sin t + H_3(s)\sin 2t\}g(\tau_2), \end{aligned}\right\} \tag{4.15}$$

where $H_3(s)$ is the solution of (4.7) and H_2 satisfies (4.6) with $f = 0$ and the relationship (4.13) holding between B_1 and η_1 in order to ensure orthogonality of the right-hand side to the eigenfunction ϕ_n of the operator on the left.

When the form (4.15) is substituted into the right-hand side of eq. (3.6) one obtains

$$\lambda_n\frac{\partial^2 u_3}{\partial t^2} + \mathrm{M}_0 u_3 =$$

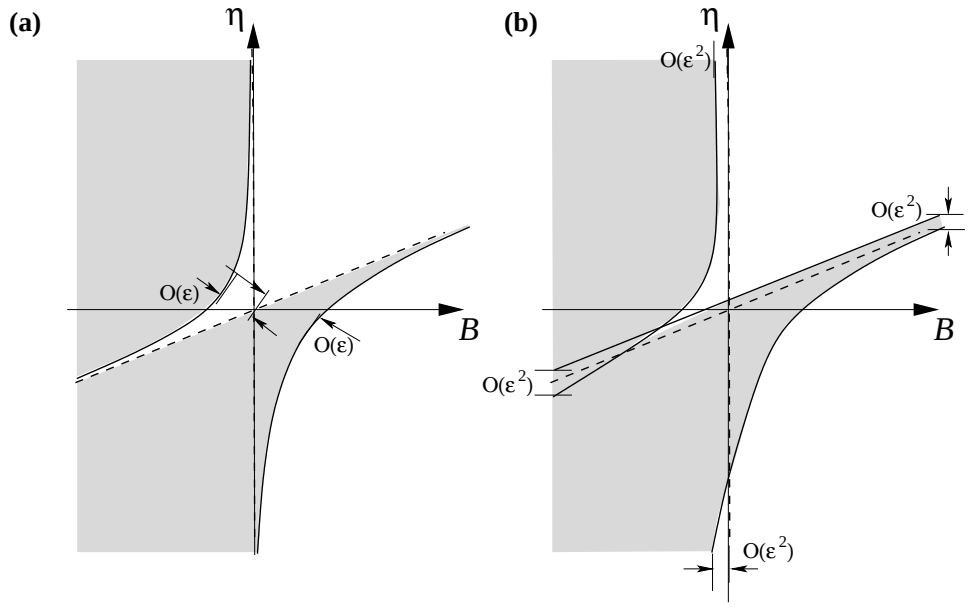

Figure 6: Schematic figure of the resonance tongue interaction process between the falling-over and first harmonic instabilities. (a) at $O(\varepsilon)$, (b) including $O(\varepsilon^2)$

$$\left\{\frac{1}{2}\lambda_n \mathrm{L}H_3 + \eta_1\left(H_2 - \frac{1}{\langle\phi_n'', \phi_n''\rangle}H_2^{IV}\right) + \eta_2\phi_n - B_2\phi_n^{IV}\right\} g(\tau_2)\sin t -$$
$$-2\lambda_n\phi_n\frac{\partial g}{\partial\tau_2}\cos t \quad + \text{ terms involving } \sin 2t \text{ and } \sin 3t, \tag{4.16}$$

where eq. (4.13) has been used to eliminate B_1 in favour of η_1 from the above equations. Finally, when we require that the right-hand-side of this equation be orthogonal to the ϕ_m we see that g must be independent of τ_2 and that

$$B_2 = \frac{1}{2}\lambda_n\frac{\langle\phi_n, \mathrm{L}H_3\rangle}{\langle\phi_n'', \phi_n''\rangle} - \eta_1\frac{\langle\phi_n, \mathrm{L}H_2\rangle}{\langle\phi_n'', \phi_n''\rangle^2} + \frac{\eta_2}{\langle\phi_n'', \phi_n''\rangle}. \tag{4.17}$$

Note that $\langle\phi_n, H_2\rangle = 0$ has been used to obtain this result.

From these results the shape of this stability-boundary in the space of the original variables B, η, ε in the neighbourhood of the singular point $(B_c, \lambda_n, \varepsilon = 0)$ can be constructed as follows:

First, note that from the power series $(3.3)_2$ we may write

$$\begin{aligned}\varepsilon\eta_1 &= (\eta - \lambda_n) - \varepsilon^2\eta_2 + O(\varepsilon^3),\\ \varepsilon^2\eta_1 &= \varepsilon(\eta - \lambda_n) + O(\varepsilon^3).\end{aligned}$$

Now, when these expressions for $\varepsilon\eta_1$ and $\varepsilon^2\eta_1$ are substituted into the above expressions

for B_1 and B_2 and the results are substituted into the series $(3.3)_3$ we obtain

$$B = B_c + \frac{(\eta - \lambda_n)}{\langle \phi_n'', \phi_n'' \rangle} - \varepsilon(\eta - \lambda_n)\frac{\langle \phi_n'', H_2'' \rangle}{\langle \phi_n'', \phi_n'' \rangle^2} + \varepsilon^2 \frac{1}{2}\lambda_n \frac{\langle \phi_n, \mathrm{L}H_3 \rangle}{\langle \phi_n'', \phi_n'' \rangle} + O(\varepsilon^3). \tag{4.18}$$

Note that the first three terms of (4.18) are precisely the expansion of the locus $B = B_{1,m}(\eta)$ up to $O(\varepsilon^2)$ that defines the condition that there is an eigenvalue $\lambda = \eta$. To see this, take $\delta = \varepsilon$, $n = m$, $\lambda = \eta$, $B_1 = B - B_c$ in (2.16) and invert the expansion up to $O(\varepsilon^2)$, noting that the equation (2.14) satisfied by f_1 is a scalar multiple of that satisfied by H_2, which is eq. (4.6) with $\eta_1 \equiv \sigma_1$ and $f = 0$. The fourth term of (4.18) is just the $O(\varepsilon^2)$ coefficient B_2^- given by (2.22) of the $\sin t$ boundary of the resonance tongue when it does not interact with the falling over mode. We conclude that this boundary of the resonance tongue does not become singular as it passes through the resonance tongue interaction point.

4.2.2 Case $\sigma_2 = 0$

On this boundary $g \equiv 0$, $f = f(\tau_2)$ and

$$h(\tau_2) = -\frac{\lambda_n B_c \langle \phi_n'', \phi_c'' \rangle}{2B_1 \langle \phi_c'', \phi_c'' \rangle} f(\tau_2) := -\frac{G_n}{B_1} f(\tau_2). \tag{4.19}$$

We require the solution to $O(1)$ even as $B_1 \to 0$ or ∞. Hence we set

$$k(\tau_2) := \sqrt{f^2 + g^2}, \quad \text{so that} \quad f = \frac{B_1}{K_n}k, \quad h = \frac{-G_n}{K_n}k, \quad \text{where} \quad K_n = \sqrt{B_1^2 + G_n^2}.$$

Also by reasoning similarly to above we may set $H_2 \equiv 0$ so that on this boundary we have

$$\left.\begin{aligned} u_1 &= (-G_n\phi_c(s) + B_1\phi_n(s)\cos t)\,\tfrac{k(\tau_2)}{K_n}, \\ u_2 &= \{H_0(s) + H_1(s)\cos t + H_3(s)\cos 2t\}\,k(\tau_2), \end{aligned}\right\} \tag{4.20}$$

where in this case

$$\mathrm{M}_0 H_0 = \frac{B_1}{K_n}\left(\frac{1}{2}\lambda_n \mathrm{L}\phi_n + G_n \phi_c^{IV}\right), \tag{4.21}$$

$$\mathrm{M}_0 H_1 - \lambda_n H_1 = \frac{1}{K_n}\left(\eta_1 B_1 \phi_n - \lambda_n G_n \mathrm{L}\phi_c - B_1^2 \phi_n^{IV}\right), \tag{4.22}$$

$$\mathrm{M}_0 H_3 - 4\lambda_n H_3 = \frac{B_1 \lambda_n}{2K_n}\mathrm{L}\phi_n. \tag{4.23}$$

When the results (4.20) are substituted into the right-hand-side of eq. (3.6) we obtain

$$\begin{aligned}
&\lambda_n \frac{\partial^2 u_3}{\partial t^2} + \mathrm{M}_0 u_3 = \\
&\quad \left\{ \frac{1}{2}\lambda_n \mathrm{L}H_1 + \frac{B_1}{2K_n}\eta_1 \mathrm{L}\phi_n - B_1 H_0^{IV} + B_2 \frac{G_n}{K_n}\phi_c^{IV} \right\} k(\tau_2) + \\
&\quad \left\{ \lambda_n \left(\mathrm{L}H_0 + \frac{1}{2}\mathrm{L}H_3 \right) + \eta_1 \left(H_1 - \frac{G_n}{K_n}\mathrm{L}\phi_c \right) - \right. \\
&\quad \left. B_1 H_1^{IV} + \frac{B_1}{K_n}\eta_2 \phi_n - \frac{B_1}{K_n} B_2 \phi_n^{IV} \right\} k(\tau_2) \cos t + \\
&\quad 2\lambda_n \phi_n \frac{B_1}{K_n}\frac{\partial k}{\partial \tau_2} \sin t \quad + \text{ terms involving } \cos 2t \text{ and } \cos 3t. \qquad (4.24)
\end{aligned}$$

Applying orthogonality conditions to the various groups of terms on the right-hand-side of this equation, we see that f is independent of τ_2, and obtain the following expressions for B_2 and η_2 in terms of B_1 and η_1:

$$B_2 = \frac{1}{2G_n\langle \phi_c'', \phi_c'' \rangle} \left(2B_1 K_n \langle \phi_c'', H_0'' \rangle - K_n \lambda_n \langle \phi_c, \mathrm{L}H_1 \rangle - B_1 \eta_1 \langle \phi_c, \mathrm{L}\phi_n \rangle \right) \qquad (4.25)$$

$$\begin{aligned}
\eta_2 = &\frac{1}{B_1}\left[\eta_1 G_n \langle \phi_c'', \phi_n'' \rangle - K_n \lambda_n \left(\langle \mathrm{L}H_0, \phi_n \rangle + \frac{1}{2}\langle \mathrm{L}H_3, \phi_n \rangle \right) \right] \\
&+ K_n \langle H_1'', \phi_n'' \rangle + B_2 \langle \phi_n'', \phi_n'' \rangle \qquad (4.26)
\end{aligned}$$

Now we have to decide how to interpret these results. At $O(\varepsilon)$ we have a neutral stability curve (4.14) in the (B, η)-plane that asymptotes to $\eta = \infty$ as $B \to 0$. However, the above formulae (4.25) and (4.26) provide corrections to both η and B_2 at each point on this curve. The most meaningful way of applying this asymptotic correction is to only take those components that are normal to the curve. To that end we can define a new co-ordinate

$$\hat{\eta} = \eta - B\langle \phi_n'', \phi_n'' \rangle,$$

so that the straight line $\eta_1 = B_1 \langle \phi_n'', \phi_n'' \rangle$ to which the curve (4.14) asymptotes as $\eta_1 \to \infty$ becomes the B_1-axis. Also, the second $O(\varepsilon^2)$-correction equation (4.26), which involves both B_2 and η_2 becomes just a condition for $\hat{\eta}_2$. Then taking B_1 as a single independent co-ordinate and, according to (4.14)

$$\hat{\eta}_1 = -\frac{\lambda_n^2 B_c^2 \langle \phi_n'', \phi_c'' \rangle^2}{2B_1 \langle \phi_c'', \phi_c'' \rangle}, \qquad (4.27)$$

we can write that the second-order corrections $\tilde{B}_2, \tilde{\hat{\eta}}_2$ should satisfy

$$(\tilde{B}_2, \tilde{\hat{\eta}}_2) = \frac{(B_2, \hat{\eta}_2) \cdot (-\hat{\eta}_1, B_1)}{B_1^2 + \hat{\eta}_1^2}(-\hat{\eta}_1, B_1) \qquad (4.28)$$

The results are presented schematically in Fig. 6(b). In order to sketch Fig. 6(b), we have used the fact that the (4.28) can be matched into the limits: **(i)** $B_1 \to 0$ (and hence $|\hat{\eta}_1| \gg 1$, but $\ll 1/\varepsilon$) and; **(ii)** $B_1 \gg 1$ (and hence $\hat{\eta}_1 \to 0$, but $B_1 \ll 1/\varepsilon$). With the correct interpretation, the former limit yields the falling-over instability boundary, whereas the latter yields the first-harmonic resonance tongue, as we now show:

(i) Consider first $B_1 \to 0$. Taking B_1 as a small parameter, then (4.27) shows $\hat{\eta}_1 = O(1/B_1)$. The leading-order term of (4.28) we then find to be in the B_2-direction and to be given by

$$\tilde{B}_2 = B_2 - \hat{\eta}_2 \frac{B_1}{\hat{\eta}_1} = -\frac{\lambda_n}{2}\langle \phi_c, LH_1\rangle - (1+B_c)G_n\langle \phi_c'', \phi_n''\rangle + O(B_1) \tag{4.29}$$

where H_1 satisfies

$$\mathrm{M}_0 H_1 - \lambda_n H_1 = -2\lambda_n B_c \langle \phi_n'', \phi_c''\rangle \phi_n - \lambda_n \mathrm{L}\phi_c + O(B_1^2). \tag{4.30}$$

Now we are interested in matching to the asymptotics of the pure falling over instability, away from the codimension-two interaction, for which ϕ_m is not a resonant mode. Setting ϕ_m to zero in (4.29) and (4.30) we obtain precisely (dropping the tilde)

$$B_2 = \frac{\lambda_n}{2}\frac{\langle LH_1, \phi_c\rangle}{\langle \phi_c'', \phi_c''\rangle}$$

which is precisely the boundary B_2^+ defined by (2.21) (with η replaced by its $O(1)$ value λ_m, for the same function H_1 where now ϕ_m is called ϕ_c) as it should be well away from the resonance interaction.

(ii) Now consider $B_1 \gg 1$. Then (4.27) shows $\hat{\eta}_1 = O(1/B_1)$. Then we find the leading-order term of (4.28) to be in the $\hat{\eta}$ direction and to be given by

$$\tilde{\hat{\eta}}_2 = \hat{\eta}_2 + O(1/B_1),$$

where $\hat{\eta}_2$ is given by the right-hand side of (4.26) without the B_2-term. Now, to match to the limit of just the $(1,n)$ resonance, away from its interaction with the falling-over instability, we must set $\phi_c = 0$, since this is no longer resonant, and also set $H_1 = 0$ since it is now resonant (it defines the coefficient of $\cos t$) and therefore can be subsumed into the $O(1)$ solution. We then obtain to leading order that (dropping tildes)

$$\hat{\eta}_2 = \eta_2 - B_2\langle \phi_n'', \phi_n''\rangle = -\lambda_n \left(\langle \mathrm{L}H_0, \phi_n\rangle + \frac{1}{2}\langle LH_3, \phi_n\rangle \right).$$

Hence, allowing η_2 to be zero, to model the codimension-one case, we get

$$B_2 = \frac{2\lambda_n}{\langle \phi_n'', \phi_n'' \rangle} \left(2\langle \mathrm{L}H_0, \phi_n \rangle + \langle LH_3, \phi_n \rangle \right),$$

where now

$$\begin{aligned} \mathrm{M}_0 H_3 - 4\lambda_n H_3 &= \frac{\lambda_n}{2} \mathrm{L}\phi_n. \\ \mathrm{M}_0 H_0 &= \frac{\lambda_n}{2} \mathrm{L}\phi_n. \end{aligned}$$

Hence we see that this is is identical to that defined by (2.21) (with H_4 now called H_0). Hence we obtain perfect matching in this case also.

4.3 Numerical evaluation

Figure 7 shows resonance tongues calculated using numerical Floquet theory with $N = 4$. Two cases of the resonance-tongue interaction studied in this section are shown corresponding respectively to the cases $n = 2$ (for which $\eta_0 = 53.285$) and $n = 3$ ($\eta_0 = 460.68$) interacting with the fundamental falling-over instability at $B_c = 0.127594$. In both cases, the general shape of the qualitative picture Fig. 6 predicted by the above theory is indeed found to occur. Specifically, we find

$$\langle \phi_c'', \phi_c'' \rangle = 12.4182, \tag{4.31}$$

$$\eta = 53.285: \quad \langle \phi_2'', \phi_2'' \rangle = 3807.01, \quad \langle \phi_c'', \phi_2'' \rangle = 8.9822 \tag{4.32}$$

$$\eta = 460.68: \quad \langle \phi_3'', \phi_3'' \rangle = 14617.8, \quad \langle \phi_c'', \phi_3'' \rangle = 6.9483. \tag{4.33}$$

Moreover we also found that the mode shape corresponding to each stability boundary is also as predicted by the analysis. The mode shape of the cosine boundary of the $(1, n)$ tongue is found to pick up a large component of the $(0, 1)$ mode as it approaches B_c, whereupon the $\phi_n \cos t$ term starts to diminish in size until, as $\eta \to |\infty|$ the mode becomes pure ϕ_c to leading-order in ε.

Note from Fig. 7(a) that there is an interaction with the $(4, 3)$-boundary for an η-value just greater than the critical one, such that at $\ll O(\varepsilon^2)$ these two boundaries exchange positions (see the inset to that figure). Similarly, in Fig. 7(b), there is an interaction between the $(1, 3)$-mode and the $(5, 3)$ at higher-order in ε (again blown up in an inset). However, the existence of these remarkably thin $(4, 3)$ and $(5, 4)$ resonance tongues makes virtually no difference to the size of the (in)stability region.

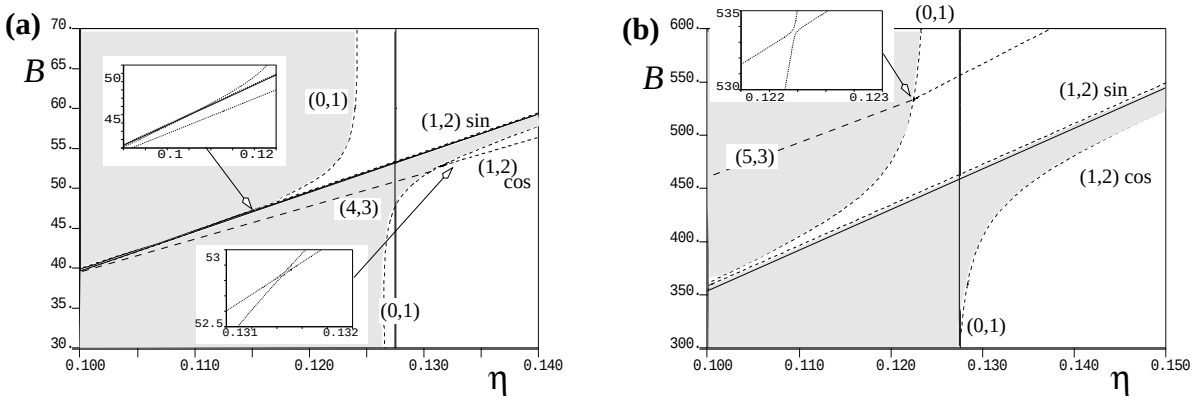

Figure 7: Numerical evaluation in the (B, η) parameter-plane of resonance tongue interaction. Solid lines depict the curves $B_{(0,1)}$ and $B_{(1,n)}$ and dashed lines represent the stability boundaries for finite ε. Shaded regions depict the areas of instability. Insets show blow ups of various regions. (a) $n = 2$, for $\varepsilon = 0.02$; (b) $n = 3$ for $\varepsilon = 0.005$.

5 The effect of damping

Let us now consider the effect on the above analysis of including damping. Recall the assumption made in Sect. 3.3 that both damping and amplitude of excitation are small parameters at $O(\delta)$, but with independent coefficients ε_1 and γ_1 to allow for the possibility of allowing one of these effects to be zero independent of the other. So we now consider the general asymptotic expansion (3.5)–(3.6) with γ_1 and ε_1 both being $O(1)$ and δ as the perturbation parameter.

5.1 Codimension-one resonances

It is well known that positive linear damping increases the size of stability regions and lifts the root points of resonance tongues off the $\varepsilon = 0$ axis (e.g. Nayfeh & Mook (1979)). In fact, damping enters at $O(\delta)$ and so makes its first non-trivial contribution in the $O(\delta^2)$ equation derived in section 3.1.1. Consider taking just a single codimension-one resonance $\eta \equiv \lambda_n/\alpha^2$. Then if $\alpha > 1/2$ we have that the $O(\delta)$ stability equation (3.23) gets replaced with the pair of equations

$$\begin{aligned} \frac{\partial g}{\partial \tau_1} + \frac{1}{2}\gamma_1 \langle \phi_n'', \phi_n'' \rangle g - K_\alpha \gamma_1 f &= 0, \\ \frac{\partial f}{\partial \tau_1} + \frac{1}{2}\gamma_1 \langle \phi_n'', \phi_n'' \rangle f + K_\alpha \gamma_1 g &= 0, \end{aligned}$$

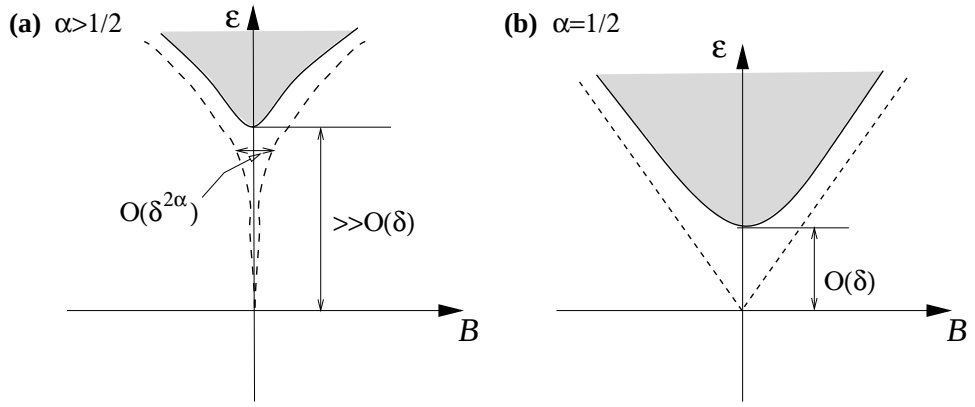

Figure 8: Sketch of resonance tongues in the presence of nonzero forcing $\varepsilon = \varepsilon_1\delta$ and damping $\gamma_1\delta$ (solid line) compared with that with $\gamma_1 = 0$ (dashed). Shaded regions correspond to instability

where now,

$$K_\alpha = -B_1 \frac{\alpha\langle\phi_n'', \phi_n''\rangle}{2\lambda_n}.$$

Note that the eigenvalues of such a system are $-(\gamma_1/2)\langle\phi_n''\phi_n''\rangle \pm iK_\alpha$, so that the origin is stable for all B_1 at this order. This shows that the resonance tongue is 'lifted off' from the $\varepsilon = 0$ axis by more than an $O(\delta)$ amount (see Fig. 8(a)).

To get a non-trivial resonance tongue at $O(\delta)$ we must consider the case $\alpha = 1/2$. Then equations (3.46) and (3.47) become (in the absence of a codimension-two interaction, so that $d = e = 0$)

$$\frac{\partial g}{\partial \tau_1} + \left(\frac{B_1\langle\phi_n'', \phi_n''\rangle}{4\lambda_n} - \frac{\varepsilon_1}{2}\langle\phi_n, \mathrm{L}\phi_n\rangle\right) f + \frac{\gamma_1}{2}\langle\phi_n'', \phi_n''\rangle g = 0, \tag{5.1}$$

$$\frac{\partial f}{\partial \tau_1} - \left(\frac{B_1\langle\phi_n'', \phi_n''\rangle}{4\lambda_n} + \frac{\varepsilon_1}{2}\langle\phi_n, \mathrm{L}\phi_n\rangle\right) g + \frac{\gamma_1}{2}\langle\phi_n'', \phi_n''\rangle f = 0. \tag{5.2}$$

When $\varepsilon_1 = 0$ the origin is stable. It becomes unstable along the neutral curve

$${\varepsilon_1}^2\langle\phi_n, \mathrm{L}\phi_n\rangle^2 = \left(\gamma_1^2 + \frac{B_1^2}{4\lambda_n^2}\right)\langle\phi_n'', \phi_n''\rangle^2, \tag{5.3}$$

which is depicted in fig. 8(b).

5.2 Codimension-two resonance tongue interaction

We can also include damping in all of the above codimension-two analyses and find its effect on resonance tongue interaction. We shall however only present the effect on the

calculation in Sect. 4, as this was the most involved and appears the most physically significant to explain the experimental results in Mullin et al. (2002). To that end, we consider u_1 given by (4.1) and see the adjustment that that the extra linear terms in (3.5)–(3.6) for non-zero γ_1 make on the stability boundaries.

Proceeding as in Sect. 4, at $O(\delta^2)$, when damping is included, eqs (4.9) and (4.10) become:

$$\begin{aligned} \frac{\partial g}{\partial \tau_1} + \frac{\gamma_1}{2}\langle \phi_n'', \phi_n'' \rangle g - \left(\frac{\eta_1}{2\lambda_n} - \frac{B_1 \langle \phi_n'', \phi_n'' \rangle}{2\lambda_n} + \varepsilon_1 \frac{\lambda_n B_c^2 \langle \phi_n'', \phi_c'' \rangle^2}{4 B_1 \langle \phi_c'', \phi_c'' \rangle} \right) f &= 0, \\ \frac{\partial f}{\partial \tau_1} + \frac{\gamma_1}{2}\langle \phi_n'', \phi_n'' \rangle f + \left(\frac{\eta_1}{2\lambda_n} - \frac{B_1 \langle \phi_n'', \phi_n'' \rangle}{2\lambda_n} \right) g &= 0. \end{aligned}$$

and eq. (4.8) is unchanged.

Writing such a system as

$$\frac{\partial g}{\partial \tau_1} + \Gamma g - ((A/B_1) + C) f = 0, \qquad \frac{\partial g}{\partial \tau_1} + \Gamma f - C g = 0, \tag{5.4}$$

where

$$\Gamma = \frac{\gamma_1}{2}\langle \phi_n'', \phi_n'' \rangle, \quad A = \frac{\varepsilon_1}{4} \frac{\lambda_n B_c \langle \phi_n'', \phi_0'' \rangle^2}{\langle \phi_0'', \phi_0'' \rangle}, \quad C = \frac{\eta_1 - B_1 \langle \phi_n'', \phi_n'' \rangle}{2\lambda_n}, \tag{5.5}$$

we note that $\Gamma > 0$ is a rescaled damping parameter and $A > 0$ is a rescaled amplitude parameter. On the other hand C can be thought of as a shifted version of η_1 so that the B_1 and C axes respectively represent the $O(\varepsilon)$ loci of the bifurcation loci $B_{0,n}$ and $B_{1,m}$.

From (5.4) and (5.5), straightforward calculation shows that the region of stability is given by

$$C(C + A/B_1) + \Gamma^2 > 0 \tag{5.6}$$

which gives the shaded region in Fig. 9. Note that in the limit $\Gamma \to 0$, we recover the undamped $O(\varepsilon)$ stability curve (4.12) sketched in Fig. 6(a). Also if $A = 0$ (corresponding to $\varepsilon_1 = 0$) then we are solving the unforced problem in the presence of non-zero damping, then the only instability is that given by B_1, which is the buckling instability $B_{0,n}$. In between these two extremes we see the curve sketched. Note that the $B_{1,m}$ tongue does not lead to an instability with finite damping at $O(\delta)$ (because of the construction in Fig. 8), but it does have a very strong influence on the shape of the falling over instability boundary. Fig. 9 also shows schematically the result of adding an $O(\delta^2)$ correction to this curve, which can be seen as a secondary effect. See Fig. 10(b) below for actual calculations of the $O(\delta)$ curves, based on the numerical evaluation of Γ, A, and C in (5.5).

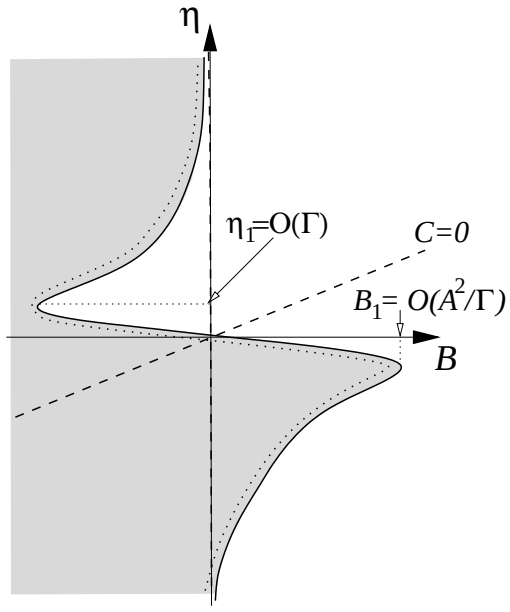

Figure 9: Schematic figure of the resonance tongue interaction process between the falling-over and first harmonic instabilities according to (5.6), in the presence of damping $\gamma_1 > 0$. Here the $O(\delta)$ curve is plotted as a solid line bounding a shaded region of instability in the (B_1, η_1)-plane. The dotted curve represent the $O(\delta^2)$ correction.

6 Experimental Comparison

In Mullin et al. (2002) the quantitative details of the experimental results using a piece of domestic curtain wire are given. A wire of critical buckling length $\ell_c = 55.3$cm is held in a clamp and subject to vertical sinusoidal oscillation with peak to peak amplitude of 2.2mm and frequency between 0 and 35 Hz. In terms of the dimensionless parameters of this paper this equates to $\varepsilon = 0.02$ and $0 < \eta < 1000$. The parameter B may be varied by allowing different lengths of wire through the holding clamp. The wire is clearly damped although it is hard to estimate the true value of the dimensionless parameter γ. It is observed that for lengths of wire a little longer than ℓ_c, $(B < B_c)$ the upright position of the wire is unstable for lower frequencies (η-values) becomes stable at higher η and becomes unstable again beyond a second η threshold. The nature of the instability at the lower-η stability boundary is a pure falling over mode ($(0, 1)$ in the notation of our theory). The upper boundary is a dynamic instability, at the same frequency of the drive, with a large component of the third spatial mode $(1, 3)$. The shape of the stability region is shown in Fig. 10. There is no evidence of any appreciable sub-harmonic instability.

Figure 10 also compares these results with two seperate theories from this paper. First in

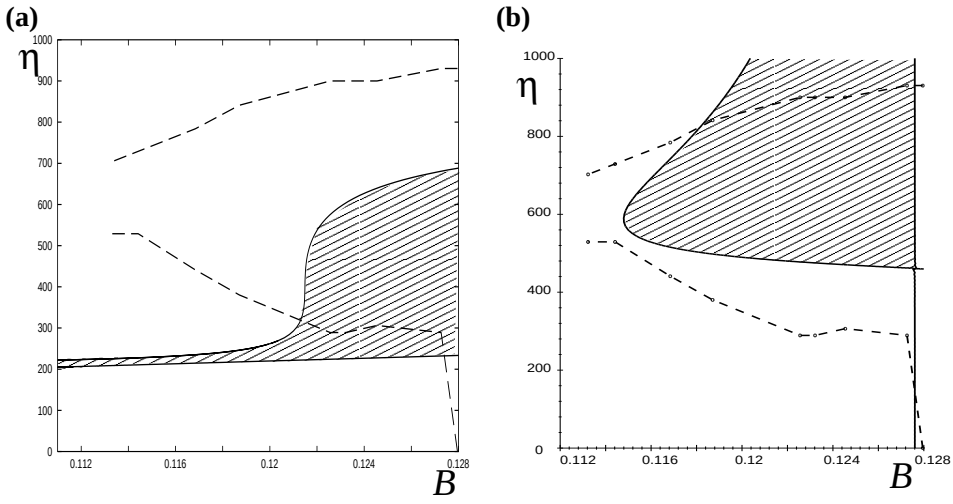

Figure 10: Comparison between theory (solid line and shading) and the experimental results of (Mullin et al. 2002) (dashed line), for the *stability* region as a function of the dimensionless parameters B and η with $\delta = 0.02$, $\varepsilon_1 = 1$. The theory is based on two different calculations close to the resonance tongue interaction between $(0,1)$ and $(1,3)$, for which $B_{0,1} = B_{1,3}$ when $\eta = \eta_0 = 460.7$. (a) Using the theoretical results from Part II, which computes the coefficients $O(\delta^2)$-coefficients B_2 and B_2^+ given by 2.18 and 2.21 which undergo singularities in accord with the theory of Sec. 4 above. In this case there is no damping. (b) Plotting the zeros of (5.6), the $O(\delta)$ coefficient of the resonance tongue interaction in the presence of damping, evaluated using the values (4.31), (4.33), with $\gamma_1 = 0.01$ being used as a representative damping value.

panel (a) we compare with the results in Sect. 4. This is essentially the same comparison that was shown in fig. 2b of Mullin et al. (2002), although in this paper we have develed a rational explanation for the resonance-tongue interaction process that underlies the shape of the stability region. Note that these results in part explain the experiments, in that the interaction between modes $(0,1)$ and $(1,3)$ lead to a wedged shape region in the (B,η)-plane.

Panel (b) compares the experimental data with the results of Sect. 5 where damping is included. Here we have used $\delta = 0.02$ with $\varepsilon_1 = 1$ and have set damping to the plausible value of $\gamma_1 = 0.01$. No other fitting is employed. Also, these results do not include any $O(\varepsilon^2)$ correction to the curves. The agreement is now very good. Note that at this level of δ, the tongue corresponding to the $(1,3)$-instability has zero width. However, its presence is strongly felt in the shape of the instability curve of the $(0,1)$ instability. In particular, the large wedge-shaped region of stability for $B > B_c$ (corresponding to the unshaded wedge within the shaded instability regions in Fig. 9) is due precisely to the resonance tongue interaction between the buckling instability and the first-harmonic resonance of the third spatial mode.

7 Discussion

The idea that parametric resonance in continuous structures can cause energy to be transfered between modes is a well established concept, due to the pioneering work of Nayfeh and collaborators (see Nayfey (2000) and references therein). This paper has expounded a somewhat different idea. Namely, the combination of resonances corresponding to different spatial modes of a structure can have surprising effects (see also (Peckham & Kevrekidis 2002) for related work that shows complex geometry of three-parameter resonance tongues; so-called *Arnol'd flames*). We have illustrated our results for the canonical model of a straight, vertically mounted elastic column subject to simple sinusoidal parametric excitation. Nevertheless many of the results are likely to have profound implications for other continuous or multi-degree of freedom problems subject to parametric excitation.

Let us summarise the main findings. First we studied the undamped problem. The key idea has been to study the genuinely three-parameter problem and to think of *each* degree

of freedom as providing a generalised Hill or Mathieu stability diagram in two parameters (B and ε). Each diagram has a buckling (zero harmonic) instability and a resonance tongue corresponding to every possible multiple of a half-frequency of the drive. The third parameter (η) we think of as sliding each of these diagrams over one another, the result being that instabilities or resonance tongues corresponding to different modes pass through eachother; i.e they *interact*. See Figs. 2 and 3.

Via multiple-scale asymptotic methods, backed up by numerical Floquet theory, we have studied each possible codimension-two interaction in detail. The cases of most interest are when the harmonic corresponding to each of the two tongues differs by unity. That is, in the notation of this paper, when $B_{\alpha,i} = B_{\alpha+1,j}$ for different spatial modes i and j. If $\alpha > 1$ then we have shown that the interaction occurs at first-order in the asymptotic parameter ε, such that there is an $O(\varepsilon)$ gap between the two instability tongues, while the width of the tongues themselves remain $\ll O(\varepsilon)$ (see Fig. 4). In fact, as can be seen from the numerically calculated Fig. 3(a) in the case of tongues $(5/2, 4)$ and $(1/2, 2)$, it appears that no two tongues that both correspond to integer (or half-integer) α and β can cross eachother, other than at $\varepsilon = 0$. There is always an interaction process where the boundary of one tongue evolves into the boundary of another with the consequent gap being $\ll O(\varepsilon)$ if $\beta \neq \alpha \pm 1$. In this problem, because the mode coupling is through a $\cos t$ term only, tongues where α and β are respectively half-integer and integer (corresponding to the existence of 4π-periodic and 2π periodic motion respectively) are unrelated and can pass through each other without interaction (see Fig. 3).

We then dealt with two special cases. The first is when $\alpha = 1/2$. Then, the leading-order resonance tongue interaction with modes for which $\beta = 3/2$ occurs at the same order as the width of the tongue. This leads to the special shape of the 2-parameter bifurcation diagram calculated and computed in Fig. 5.

The main special case we studied, in Sec. 4 is that for which $\alpha = 0$, corresponding to a static buckling instability of the column. Here surprising things happen near η-values for which a pure harmonic instability $\beta = 1$ occurs for the same B-value when $\varepsilon = 0$. In particular we showed that the cosine boundary of the harmonic tongue and the buckling instability curve which are both ordinarily quadratic in ε, undergo a singularity of their $O(\varepsilon^2)$-coefficients which we have resolved in a new form of asymptotic expansion. The result is the shapes of the instability regions shown in Figs. 6 and 7, which has a large 'blob' of stability above the line $B = B_{1,j}$ for $B < B_c$ and a corresponding area of

instability below $B = B_{1,j}$ for $B > B_c$. It is this blob of stability which we claim explains the qualitative shape of the stability region in the curtain-wire experiment reproduced in Fig. 10(a).

To get qualitative agreement with the experiments though, we found it necessary to include material damping. It is well known that linear damping lifts resonance tongues off from zero amplitude in Mathieu-type stability diagrams, and this problem is no exception (Fig. 8). The key to understanding the experimental parameter regime though, is to include damping in the interaction between the buckling instability and the harmonic resonance. This lead to the asymptotic results in Sec. 6, which according to Fig. 10(b) gives good quantitative agreement with the experiments.

Now, as remarked in the conclusions to our earlier papers, we are really only scratching at the surface of the complete nonlinear dynamics of a parametrically excited vertical column. In Part *II* we showed how to introduce a nonlinear formulation of the problem, which leads to a differential algebraic equation formulation, with the tension in the column acting as a Lagrange multiplier. Also, as remarked in (Mullin et al. 2002), the curtain wire used in the experiment is anything but linearly elastic. Even for the one-degree-of freedom simple pendulum under parametric excitation the dynamics of the fully nonlinear system are remarkably rich (van Noort 2001). For small amplitude nonlinear motion in a neighbourhood of the codimension-two instabilities we study, one could presumably infer information on the presence of (both rotating and oscillating) periodic and quasi-periodic solutions from a centre manifold and normal form approach, e.g. as in (Dangelmayr, Fiedler, Kirchgässner & Mielke 1996). Yet, even for the linear problem we have studied we have not explored the implications of many finite-amplitude effects such as the 'pinching off' of resonance tongues which seemed to occur as a consequence of the interaction between (α, i) and $(\alpha + 1, j)$ resonance tongues for $\alpha > 1$, as was remarked upon in Sect. 3. There are also questions of rigour that we have not addressed. Even for one-degree-of-freedom parametrically excited systems, whether linear stability implies nonlinear stability is a non-trivial question (Bartuccelli, Gentile & Georgiou 2002). There are also clearly small-divisor problems, and KAM-theory may be able to shed some light, see for example the book by Kuksin (1993) for infinite dimensional systems.

Nevertheless we hope that this paper has provided a rational and mathematically consistent explanation for the 'upside down' stability of a wire under vertical excitation, previously reported in the popular media (e.g. Acheson & Mullin (1998)). More seri-

ously, we have explained what we believe to be a new universal mechanism for creation of finite regions of stability (and instability) in parametrically excited systems. Importantly this does *not* involve sub-harmonic resonance, but the interaction of first-harmonic resonance with a steady-state instability.

References

Acheson, D. (1997), *From Calculus to Chaos, An Introduction to Dynamics*, Oxford University Press, Oxford.

Acheson, D. & Mullin, T. (1998), 'Ropy magic', *New Scientist* **February**, 32–33.

Bartuccelli, M. V., Gentile, G. & Georgiou, K. V. (2002), 'On the stability of the upside-down pendulum with damping', *Proc. Roy. Soc. Lond. A* **458**, 255–269.

Broer, H. & Levi, M. (1995), 'Geometrical aspects of stability theory for Hills equations', *Arch Ration Mech An* **131**, 225–240.

Champneys, A. & Fraser, W. (2000), 'The 'indian rope trick' for a continuously flexible rod; linearized analysis', *Proc. Roy. Soc. Lond. A* **456**, 553–570.

Dangelmayr, G., Fiedler, B., Kirchgässner, K. & Mielke, A. (1996), *Dynamics of nonlinear dissipative systems: reduction, bifurcation and stability*, Longman, Harlow, U.K. Pitman Research Notes in Mathematics Series, no. 352.

Fraser, W. & Champneys, A. (2002), 'The 'indian rope trick' for a parametrically excited flexible rod: nonlinear and subharmonic analysis', *Proc. Roy. Soc. Lond. A* **458**, 1353–1373.

Galan, J., Fraser, W., Acheson, D. & Champneys, A. (2002), 'The parametrically excited upside-down rod: an elastic jointed pendulum model'. To appear in *J. Sound Vibration.*

Greenhill, A. (1881), 'Determination of the greatest height consistent with stability that a pole or mast can be made ...', *Proceedings of the Cambridge Philosophical Society* **IV** Oct 1880 – May 1883, 65–73.

Jordan, D. W. & Smith, P. (1986), *Nonlinear Ordinary Differential Equations* (2nd Edition) , Oxford University Press, Oxford.

Kuksin, S. (1993), *Nearly integrable infinite-dimensional Hamiltonian systems*, Springer-Verlag, Berlin. Lecture Notes in Mathematics, 1556.

Mullin, T. Champneys, A., Fraser, W., Galan, J. & Acheson, D. (2002), 'The 'indian wire trick' by parametric excitation check new title'. To appear in *Proc Roy Soc Lond A*.

Nayfeh, A. & Mook, D. (1979), *Nonlinear Oscillations*, Wiley Interscience, New York.

Nayfey, A. (2000), *Nonlinear Interactions: Analytical, Computational and Experimental Methods*, Wiley Interscience, New York.

Peckham, B. & Kevrekidis, I. (2002), 'Lighting Arnold flames: resonance in doubly forced periodic oscillators', *Nonlinearity* **15**, 405–428.

van Noort, M. (2001), The parametrically forced pendulum. A case study in 1 $\frac{1}{2}$ degree of freedom, PhD thesis, RU Groningen.